DEUTSCHES ELEKTRONEN-SYNCHROTRON DESY

DESY 78/42
August 1978

THE NEW HEAVY LEPTON τ

by

Günter Flügge

NOTKESTRASSE 85 · 2 HAMBURG 52

To be sure that your preprints are promptly included in the
HIGH ENERGY PHYSICS INDEX ,
send them to the following address (if possible by air mail) :

DESY
Bibliothek
Notkestrasse 85
2 Hamburg 52
Germany

THE NEW HEAVY LEPTON τ

by

Günter Flügge
Deutsches Elektronen-Synchrotron DESY, Hamburg

Abstract:

Experimental evidence for the production of the heavy lepton τ in e^+e^- annihilation and the determination of its properties are reviewed. All data are in good agreement with the predictions of the heavy lepton hypothesis.

THE NEW HEAVY LEPTON τ

CONTENTS

I. INTRODUCTION

The problem of heavy leptons is as old as the discovery of the muon, the twin brother of the electron. It is well known that these two particles - called leptons - are identical except for their masses and their lepton numbers. The latter manifests itself in as much as the neutral partners - the neutrinos - associated with electrons and muons are different from each other. It has been an ardent question in high energy physics, why the muon exists and whether there are more even heavier leptons.

In the standard model of unified weak and electromagnetic interactions /1/ left-handed leptons and quarks come in (iso) doubletts,

$$\text{leptons} \quad \begin{pmatrix} \nu_e \\ e^- \end{pmatrix} \quad \begin{pmatrix} \nu_\mu \\ \mu^- \end{pmatrix} \qquad \text{quarks} \quad \begin{pmatrix} u \\ d_c \end{pmatrix} \quad \begin{pmatrix} c \\ s_c \end{pmatrix} \tag{1}$$

where $d_c = s \cdot \sin\theta_c + d \cdot \cos\theta_c$, $s_c = s \cdot \cos\theta_c - d \cdot \sin\theta_c$, θ_c = Cabibbo angle.

This remarkable symmetry between these supposedly basic constituents of matter was predicted in 1964 and further supported by the "GIM" mechanism /2/. Ten years later with the discovery of "charm", this idea found its splendid confirmation /3/.

Although there are good reasons why the number of leptons and quarks should be equal /4/ a deeper understanding of this symmetry - if it exists in nature - has not been found yet. Nevertheless, one will be reluctant to abandon this symmetry just acquired.Therefore the discovery of new quarks or leptons will immediately raise suspicion that the other "sector" may be larger, as well. In fact, after the discovery /5/ and confirmation /6/ of a new lepton at SLAC and DESY between 1975 and 1977 it took less than two years to see first experimental hints towards new quarks from a muon pair resonance at FNAL /7/. In May 1978 finally the confirmation of this resonance in e^+e^- annihilation and thereby the discovery of

a new quark could be announced at DESY /8/. This new quark, which reveals itself through a narrow resonance at 9.46 GeV, is most likely of the "beauty" type. The above symmetry can now be tentatively extended to

$$\text{leptons} \quad \begin{pmatrix} \nu_e \\ e^- \end{pmatrix} \begin{pmatrix} \nu_\mu \\ \mu^- \end{pmatrix} \begin{pmatrix} \nu_\tau \\ \tau^- \end{pmatrix} \qquad \text{quarks} \quad \begin{pmatrix} u \\ d_c \end{pmatrix} \begin{pmatrix} c \\ s_c \end{pmatrix} \begin{pmatrix} t \\ b \end{pmatrix} \tag{2}$$

with the new quark flavours t (truth) and b (beauty).

The purpose of this paper is to collect the evidence for the new heavy lepton τ /9,10,11,12/ and its decay properties at a time, where the experimental data present a convincing and rather complete picture.

The paper is organized in the following way: After explaining possible signatures for the new particle in Section II, a short description of relevant experiments is given in Section III. Experimental data are presented in Section IV showing clear evidence for a new lepton. The decay properties of this new particle are then discussed in Section V and the data are summarized in Section VI.

II. SIGNATURES FOR HEAVY LEPTONS

1. Production

A variety of processes has been discussed for a potential production of heavy leptons /9/. The simplest one is the electromagnetic pair production through a virtual or real photon. Among many possible mechanisms like photon and lepton production, Drell-Yan process and e^+e^- annihilation, the latter one offers several advantages.

The total cross section for e^+e^- annihilation which sets the scale for background reactions is of the same order as the leptonic cross section, whereas it is orders of magnitude higher in the other reactions. Together with the easy and well defined production kinematics, this makes e^+e^- machines a unique tool to search for heavy leptons, provided the center of mass energy is sufficiently high.

Not only is the process of e^+e^- annihilation into new leptons simple from the experimental point of view, it can also be predicted with certainty in all details by quantum electrodynamics (QED). For the production of a pair of pointlike spin 1/2 particles $\tau^+ \tau^-$ we get

$$\sigma_{\tau\tau} = \sigma_{\mu\mu} ((3\beta - \beta^3)/2) \qquad (3)$$

where

$$\sigma_{\mu\mu} = (4\pi \alpha^2)/(3 s) = 21.71 \text{ nb}/E_b^2 \qquad (E_b = s^{1/2}/2 = \text{beam energy})$$

is the cross section for $e^+e^- \rightarrow \mu^+\mu^-$ and

$$\beta = (1 - M_\tau^2/E_b^2)^{1/2} \qquad (M_\tau = \text{mass of } \tau)$$

is the velocity of τ. $\sigma_{\tau\tau}$ rises quickly from the threshold at $s^{1/2}=2M_\tau$ and approaches $\sigma_{\mu\mu}$ asymptotically. Therefore, one often uses the ratio

$$R_\tau = \sigma_{\tau\tau}/\sigma_{\mu\mu} \qquad (4)$$

to describe the cross section.

In this context, one should recall briefly the central role of $\sigma_{\mu\mu}$ for all e^+e^- annihilation processes. According to common belief hadronic e^+e^- reactions proceed mainly through the production of a quark-antiquark pair which fragments into hadrons. Since one assumes quarks to be pointlike spin 1/2 particles, the hadronic production is given by

$$\sigma_{had} = \sum_q Q_q^2 \sigma_{\mu\mu} = \sigma_{\mu\mu} (\sum_q Q_q^2) \qquad (5)$$

where the sum goes over all types of quarks. Again, the quantity

$$R = \sigma_{had}/\sigma_{\mu\mu} = \sum_q Q_q^2 \qquad (6)$$

is frequently used to describe e^+e^- annihilation into hadrons. The sum is readily predicted from the quark model. In table 1 R is calculated for different quark flavours, with and without colour.

2. Decay

Many models with new heavy leptons have been described. Several of these will be discussed later in the interpretation of data. The conceptually simplest and in many ways most persuasive model of sequential heavy leptons - which will finally turn out to offer the best description of the data - will be discussed in some detail.

This "standard model" assumes a new heavy lepton continuing the sequence of electron and muon as described in the introduction. This new lepton participates in the weak interaction in the same way as the other two. The leptonic weak current in the Lagrangian

$$= G/2^{1/2} \; J_\alpha^+ \; J_\alpha^- \qquad (7)$$

can then be written as

$$J_\alpha^{\ell^+} = \bar{\nu}_e \, \gamma_\alpha(1 - \gamma_5) \, e^- + \bar{\nu}_\mu \, \gamma_\alpha(1 - \gamma_5) \, \mu^- + \bar{\nu}_\tau \, \gamma_\alpha(1 - \gamma_5) \, \tau^- \qquad (8)$$

assuming V-A structure of the new current and a new massless neutrino.

In this model, leptonic decays of τ into e and μ are readily calculated. If the new particle is heavy enough[+)] it will also decay semihadronically. Table 2 gives the branching ratios /14/ for a lepton mass of 1.8 GeV/c^2. Details of the calculation will be discussed in section V.

Table 2 shows that most decays (about 70 %) are characterised by one single charged particle in the final state. In nearly half of the cases these are electrons or muons. Several neutrinos in each reaction will show up as large missing energy. Consequently, the following signatures will be appropriate for a heavy

[+)] Previous measurements at ADONE /13/ limit the mass to $\geq$1.15 GeV/c^2.

lepton search

$$\begin{aligned} &\text{(i)} \quad e^+e^- \rightarrow \text{two charged particles} + \text{missing energy} \\ &\text{(ii)} \quad \rightarrow \text{one charged lepton} + \text{missing energy} \\ &\text{(iii)} \quad \rightarrow \text{two charged leptons} + \text{missing energy} \end{aligned} \tag{9}$$

In this sequence, selectivity rises with falling cross section. The first evidence for a new lepton came in fact from a special choice of dilepton events (iii), namely /5/

$$e^+e^- \rightarrow \mu^{\pm} e^{\mp} + \text{missing energy}. \tag{10}$$

Most knowledge about the new particle, however, was later extracted from inclusive lepton data (ii).

3. Competing processes

To understand the experimental problems a discussion of two kinds of processes in e^+e^- annihilation is necessary, which may fake the signatures of heavy leptons.

QED

From quantum electrodynamics (QED) a number of reactions is known to contribute to these signatures. Besides the collinear ee and $\mu\mu$ final states, radiative processes $e^+e^- \rightarrow e^+e^-\gamma$, $\mu^+\mu^-\gamma$, $e^+e^-\gamma\gamma$, and $\mu^+\mu^-\gamma\gamma$ have to be eliminated. In addition two-photon processes of the type $e^+e^- \rightarrow e^+e^-$ + X have to be taken into account. For instance the reaction $e^+e^- \rightarrow \mu\mu ee$ may fake signature (10) if a μe pair escapes detection.

Charm

Another important source of competing processes is the production and decay of charmed mesons /15/ above a threshold of about 3.7 GeV in $s^{1/2}$.

A comparison of production and decay mechanisms yields considerable differences between charm and heavy leptons. While leptons are produced elastically, only the basic quark-antiquark process is elastic for charm mesons. The subsequent fragmentation will generally proceed through cascades of excited mesons and result in an inelastic pair production of the weakly decaying charm meson ground state.

Consequently, the multiplicity will be larger and the mean energy of charm particles smaller than in the heavy lepton case. These differences will even be enhanced by the weak decay process. Charm couples to s and d quarks according to the GIM mechanism while the τ couples to a neutrino in its weak current. This tends to increase the differences in multiplicities. Furthermore, the leptonic decay will be pointlike, whereas the charm decay involves a form factor. This form factor and the larger mass of the decay products will result in a relatively soft lepton spectrum in charm decays /16/.

In conclusion, mainly two criteria will be selective for heavy leptons against charm,

low multiplicity and

hard lepton spectrum.

III. DETECTORS

In this chapter experiments which have provided major contributions to the heavy lepton data will be discussed in some detail. They were performed at the double storage ring DORIS at DESY and the SPEAR storage ring at SLAC, respectively. Somewhat arbitrarily they will be grouped into those with prominent electron or muon identification.

Muon identification

PLUTO

A cross section of the solenoidal detector PLUTO /17/ at DORIS is shown in Fig. 1. The superconducting coil, which produces a magnetic field of 2 T, is filled with

a set of 14 cylindrical proportional chambers, allowing for track reconstruction over 87 % of 4π. A lead cylinder of .44 radiation lengths behind the 8th chamber and another one of 1.7 radiation lengths behind the 12th chamber provide photon and electron identification. The outer lead cylinder followed by two proportional chambers can specifically be used for shower recognition over 55 % of 4π. Electron identification is thus accomplished with an efficiency of 85 % (above 600 MeV electron energy) and a hadron misidentification probability

$$P(h \to e) = (3.5 \pm 0.7)\ \%.$$

Additional proportional tube chambers outside the iron yoke allow for muon identification over 45 % of the polar angle range $|\cos\theta| < .75$. Hadron misidentification was measured to be

$$P(h \to \mu) = (2.8 \pm 0.7)\ \%.$$

SLAC-LBL

Fig. 2 shows the SLAC-LBL detector /18/ at SPEAR, which is again of the solenoidal type. The field of the warm coil is .4 T. Four double layers of spark chambers are used for track reconstruction over 70 % of the solid angle. A lead scintillation shower counter outside the coil provides modest shower resolution and therefore large hadron misidentification of $P(h \to e) \approx 18$ % over 65 % of 4π. Spark chambers outside the 20 cm thick iron yoke allow for muon identification with $P(h \to \mu) \sim 20$ % at a momentum cutoff of 600 MeV/c.

The "muon tower" on top of the detector offers a much better muon identification with $P(h \to \mu) = 2.8$ % with a momentum cutoff of 900 MeV/c, over 8.8 % of 4π.

Two other experiments at SPEAR have contributed to the τ search, the Maryland-Pavia-Princeton-Stanford Collaboration /19/ (MPPS) and the Ironball /20/.

Electron Identification

Lead-Glass Wall

In 1977 the SLAC-LBL detector was operated in a modified version, the "Lead-Glass Wall" extension /21/. Two layers of lead-glass counters interleaved with spark chambers covered $\pm 20^{\circ}$ in azimuthal and $\pm 30^{\circ}$ in polar angle. Good energy resolution and accordingly low hadron misidentification of $P(h \rightarrow e) = 2$ % were combined with a good electron detection efficiency of 89% above 400 MeV/c momentum.

DASP

Fig. 3 shows the DASP detector /16,22/ at DORIS. The non-magnetic inner detector, which is moved from its central position in the drawing, covers 70 % of 4π. It consists of lead-scintillator and lead-proportional tube sandwiches. Two identical spectrometers at large angles provide excellent momentum resolution and particle identification through Čerenkov, time-of-flight, shower counter and range counter techniques. This allows for electron identification down to 200 MeV/c momentum. The solid angle is however restricted to two times 3.6 % of 4π.

DELCO

The DELCO detector /23/ shown in Fig. 4 was operated at SPEAR since 1977. It was specially built for good electron identification, which is accomplished by Čerenkov and shower counters over 65 % of the solid angle. This combination provides an excellent hadron rejection of $P(h \rightarrow e) < 0.05$ %. A small magnetic inner detector allows for reasonable momentum measurement over about 60 % of 4π.

DESY-Heidelberg

The DESY-Heidelberg detector /24/ (Fig. 5) is a powerful device for electron and photon detection with sodium iodide and lead-glass counters covering 86 % of 4π.

Muons can be identified by traversing 4.6 collision length and being detected in drift chambers over 55 % of 4π. A small non-magnetic inner detector covers 86 % of the full sphere.

IV. EVIDENCE FOR THE PRODUCTION OF A NEW HEAVY LEPTON

In this chapter a survey of the relevant data will be given. The presentation will not follow the historical development but rather proceed in order of increasing evidence.

1. Total Cross Section

First of all let us see whether the total cross section data allow a new particle. Asymptotically, a new lepton would contribute nearly one unit in R to the hadronic cross section (pure leptonic events are expected at a level of less than 10 %). Total cross-section data are available from the SLAC-LBL /25/, PLUTO /26/ and DASP /27/ collaborations. As an example, the PLUTO data are shown in Fig. 6. A comparison with the prediction of the quark model (Table 1) shows that above charm threshold the increase expected from a new quark is not sufficient to describe the data. On the other hand, inclusion of a new lepton contribution yields much better agreement. The remaining difference of .3 to .5 units in R stays within the systematic uncertainties of the measurement and the prediction (gluon corrections) /28/. The other three experiments yield even higher cross sections and therefore demand even more a new particle.

2. Inclusive Lepton Data

As shown in Table 2, the new lepton is expected to decay into electrons and muons with considerable branching ratios. Consequently, it should show up in an excess of "anomalous" lepton events above threshold.

a) Inclusive Muon Production

Three collaborations - MPPS /19/, SLAC-LBL /29/ and PLUTO /6,30/ - have measured inclusive muon production in the reaction

$$e^+ e^- \rightarrow \mu^{\pm} + X, \tag{11}$$

where X stands for at least one charged particle. The muon momentum cutoff varies between 0.9 and 1.05 GeV/c. Experimental details are very similar for all three sets of data. Since the strongest signal is expected at low multiplicities (section II), data are subdivided into a twoprong and a multiprong sample. In the twoprong class, an acoplanarity cut[+)] is applied to suppress QED contributions and cosmic ray background.

In both classes, events with low missing mass are removed, which again suppresses QED events and favours events with several neutrinos. The final signal events are thus

twoprongs: $e^+e^- \rightarrow \mu^{\pm}$ + 1 track + missing mass (12)

multiprongs: $e^+e^- \rightarrow \mu^{\pm}$ + $\geq$ 2 tracks + missing mass (13)

These samples have still to be corrected for (small) residual QED contributions /31/ and background of hadrons faking a muon by decay or by punching through the iron. Contributions from J/ψ production were studied in the PLUTO detector and turned out to be small /32/.

Fig. 7 shows the results for the remaining anomalous muon production in the twoprong and multiprong class. The cross sections are scaled to the same momentum cutoff of 1 GeV/c (cf. figure caption). All data are in perfect agree-

[+)] The acoplanarity is defined by the difference in azimuthal angle between the two tracks.

ment. The curve is a fit of the "standard model" to the PLUTO data. It extrapolates very nicely into the high energy point in the twoprong case. For multiprongs however, the 7 GeV point is considerably higher, probably due to charm contributions at these energies. The energy dependence of the cross section is in good agreement with the expectation for pair production of point-like spin 1/2 particles and notably excludes boson pair production. From the threshold behaviour of the inclusive muon data a rough determination of the mass can be achieved with

$$M_\tau = (1.9 \pm .1)\ \mathrm{GeV}/c^2.$$

The error is mainly due to the high momentum cutoff which results in low statistics and large extrapolation uncertainties for the low energy part of the momentum distribution. To do better, one has to use electrons which allow for a much lower momentum cutoff.

b) Inclusive Electron Production

Inclusive electron production has been measured by four collaborations - DASP /27/, DELCO /33/, Lead-Glass Wall /34/ and DESY-Heidelberg /35/ (the latter measured muon production as well). Electrons were identified by Čerenkov, time-of-flight and different shower-counter techniques as described in Sec.III. The lowest electron momenta thus available were 200 MeV/c (DASP), 300 MeV/c (DELCO), 400 MeV/c (SLAC-LBL) and 500 MeV/c (DESY-Heidelberg). Since generally charm decays will dominate low momenta and large multiplicities, only twoprong events were considered. To suppress Bhabba scattering the events were required to contain a second non-showering track. The signature chosen was thus

$$e^+e^- \rightarrow e^\pm + \text{non showering track} + \geq 0 \text{ photons} \qquad (14)$$

(The DESY-Heidelberg group restricted its data sample to events without photons.) For the same reason as discussed for muon events, large missing mass and acoplanarity of the

two tracks were required in all experiments. The remaining background from beam gas events, charm production, QED events and electron misidentification is small, typically 5 to 10%. The DASP group was the first one to show that τ production is present on the $\psi'(3.7)$ resonance /27/. An excessive hadronic background and electrons from cascade decays rendered this measurement more difficult than at higher energies. This DASP result was a major breakthrough not only for the mass determination. Even more important it proved conclusively that the τ is produced below charm threshold and that an association with charm is definitely excluded. DESY-Heidelberg and DELCO followed quickly, measuring τ production even below the ψ' resonance /33,35/.

Figs.8, 9 and 10 show the energy dependence of the cross sections, for DASP, DELCO and DESY-Heidelberg, respectively. (The Lead-Glass Wall experiment has lower statistics near threshold). All results indicate a smooth behaviour of the cross section, as expected from heavy lepton production. The DELCO data in particular give a convincting account of the predicted energy dependence of the cross section. Like for muons, the data again argue clearly against spin 0 or spin 1 particle production. From these measurements the mass of the τ is determined to be (assuming V-A coupling of the τ decay):

$M_\tau = (1.807 \pm .020)$ GeV/c^2 DASP /27/

$M_\tau = (1.790 + .007, - .010)$ GeV/c^2 DESY-Heidelberg /35/

$M_\tau = (1.782 + .002, - .007)$ GeV/c^2 DELCO /33/

3. Dilepton Events

Another major source of information are dilepton events which occur through the reaction

$$e^+ e^- \rightarrow \tau \tau \quad \begin{matrix} \longrightarrow \ell\nu\nu \\ \longrightarrow \ell\nu\nu \end{matrix} \qquad \ell = e, \mu \qquad (15)$$

In particular the process

$$e^+ e^- \rightarrow \mu^{\pm} e^{\mp} + \text{missing energy} \qquad (16)$$

lead to the first observation /5/ of τ production by its striking signature of large missing energy and apparent lepton number non-conservation in the observed μe final state. As an example Fig. 11 demonstrates the appearance of such an event in the PLUTO detector. The signatures of a muon and an electron and the momentum imbalance are clearly visible. Table 3 summarises the available data. The historically first sample of events from SLAC-LBL still suffered from a relatively large background due to moderate e and μ identification (section II). Results from PLUTO /6/ and later from the Lead-Glass-Wall /34/ and DASP /27/ were complementary to the SLAC-LBL data in the sense of very low background at the expense of low statistics. They fully confirmed the original interpretation of the data as originating from τ production. Fig. 12 and 13 show the SLAC-LBL and PLUTO μe-cross section as a function of energy, the latter again compared with the inclusive μ data. They all show the expected threshold behaviour.

Undetected Particles

The high missing mass of μe events (typically $MM^2 > 3$ $(GeV/c^2)^2$) and the large missing energy (typically $> s^{1/2}/2$) already suggest the presence of at least two undetected particles (or one with high mass). Furthermore, from the momentum spectra we concluded that the leptons are accompanied by two other particles (section IV.4).

To determine the nature of those undetected particles experimentally, let us consider reactions of the type

$$e^+ e^- \rightarrow \mu^{\pm} e^{\mp} + X \qquad (17)$$

where X are ≥ 2 charged particles, photons or π^0's. Of course, these events should be absent, if the standard heavy lepton hypothesis is right. In fact, from upper limits on these processes the probability can be estimated that the eμ events are faked by events of type (17) with X escaping the detector. The PLUTO experiment gives the lowest upper limit of 9% (90% C.L.) including the most dangerous case, where two K^0's are produced /6/.

Consequently, in most of the events the additional particles have to be neutrinos or neutrons. From the shape of the momentum distribution, an upper limit of 250 MeV/c^2 can be set on the mass of the neutral particles involved (section V.2). This excludes the neutron and we are only left with neutrinos to explain the missing energy.

Collinearity

Elastic production of a pair of heavy particles is clearly supported by the observed threshold behaviour. Another manifestation of this production mechanism is that the decay products of the two heavy leptons are forced back to back by the momentum boost. This is nicely demonstrated in Fig. 14 for the μe events from SLAC-LBL /5/. The collinearity distribution of the two leptons in fact shrinks with increasing energy, again in good agreement with the quantitative predictions of the standard model.

4. Momentum Distributions

If the observed leptons originate from the decay of heavy leptons, their decay characteristics should be completely independent of the special type of event.

$$e^+ e^- \rightarrow \tau^+ \tau^- \quad \begin{cases} \tau^+ \rightarrow \mu^+ \nu\bar{\nu},\ e^+ \nu\bar{\nu} \\ \tau^- \rightarrow \text{something} \end{cases} \qquad (18)$$

In particular, the lepton momentum distributions in reactions (12), (13), (14) and (16) should be the same. Moreover, the shape of the distributions can be calculated /36/.

Figs. 15 to 19 show momentum distributions for both electrons and muons for all event classes. In all figures, the full lines represent fits to the data with the standard assumptions for heavy leptons.

The comparison is convincing: all data show in fact the same characteristics

- the spectra are relatively hard (compared to spectra from charmed particles)
- they are independent of the specific final state,
- they are all well described by 3-body decay of the standard heavy lepton model,
- 2-body decay is ruled out.

V. DECAY PROPERTIES OF THE NEW HEAVY LEPTON

Throughout section IV we have seen overwhelming evidence that a new pointlike spin 1/2 particle τ is produced in pairs in e^+e^- annihilation. The mass of this new heavy lepton is

$$M_\tau = (1.782\ ^{+.002}_{-.007})\ \text{GeV}/c^2. \qquad (19)$$

This chapter will be devoted to a discussion of its decay properties. Data will be compared with the predictions of a "standard model" of a heavy sequential lepton of mass 1.8 GeV/c^2 taking part in the conventional weak interaction through a (V-A) coupling to its own massless neutrino.

1. Lifetime

In this model, the lifetime is calculated as /14/

$$\tau_\tau = BR(\tau\to e\nu\nu)(M_\mu/M_\tau)^5 \cdot \tau_\mu = 2.8 \times 10^{-13}\ s \qquad (20)$$

where τ_μ and M_τ are the lifetime and mass of the muon. The corresponding decay length is less than a tenth of a mm and cannot be measured in any of the existing detectors. However, from a study of the closest distance at which tracks approach the beam axis, an upper limit can be inferred:

$\tau_\tau < 11 \cdot 10^{-12}$ s (95 % C.L.) SLAC-LBL /11/

$\tau_\tau < 3.5 \cdot 10^{-12}$ s (95 % C.L.) PLUTO /37/

2. Leptonic Decays

The partial width for leptonic decays (Fig. 20a)

$\tau \to e\ \nu\nu$

$\tau \to \mu\ \nu\nu$

can be calculated in the standard model. They differ only by a small phase-space correction. From a computation of the other semihadronic decays (section V.3), the branching ratios of Table 2 can be obtained. These branching ratios have been determined in various experiments as listed in Table 4. The "world average" of

$$BR(\tau\to\ell\nu\nu) = (16.7 \pm 1.0)\ \% \qquad (21)$$

is in good agreement with the theoretical prediction. The relative strengths of μ and e decays have been checked by DASP, PLUTO and SLAC-LBL and found to be equal within the rather large experimental errors: $B_\mu = BR(\tau\to\mu\nu\nu)$, $B_e = BR(\tau\to e\nu\nu)$

$B_\mu/B_e = .92 \pm .32$ DASP /27/

$B_\mu/B_e = .92 \pm .37$ PLUTO /6/

$B_\mu/B_e = 1.40 \pm .48$ SLAC-LBL /38/

$B_e/B_\mu = 1.12 \pm .48$ SLAC-LBL /38/

The form of the leptonic spectrum can be calculated from the standard model as well. As we have seen in section IV, all distributions are in reasonable agreement with the expectation. To be more specific, one can allow for an arbitrary mixture of V and A pieces in the weak τ current

$$J_\alpha^{\tau^+} = \nu_\tau \gamma_\alpha \left[\sin\delta(1 - \gamma_5) + \cos\delta(1 + \gamma_5)\right] \tau^- \qquad (22)$$

and for neutrino masses $m_{\nu_\tau} \neq 0$. Variations in δ and m_{ν_τ} will show up in the detailed form of the leptonic spectra.

The SLAC-LBL /11/, PLUTO /6/ and DELCO groups have analysed their data with respect to a V±A form of the weak interaction. All three experiments favour V-A. The clearest evidence (Fig.16) is given by DELCO which measures the Michel parameter as

$$\delta = .66 \pm .13 \quad \text{DELCO /12/}$$

compared to an expectation of .64 for V-A and -.17 for V+A (without radiative corrections). Note, however, that pure V and A structures lie in between V± A and cannot be ruled out by present data.

Upper limits on the neutrino mass have been determined by SLAC-LBL (< 600 MeV/c^2) /29/ and PLUTO (< 300 MeV/c^2) /39/. The best value, recently obtained by DELCO, is

$$M_{\nu_\tau} < 250 \text{ MeV}/c^2 \quad (90\ \%\ \text{C.L.}) \qquad \text{DELCO /12/.}$$

3. Semihadronic Decays

Since the τ mass is high enough to allow for semihadronic decays (Fig. 20B), we have an excellent tool to check whether the new particles do in fact participate in the conventional weak interaction of the standard model. If this

is the case, it should couple to two kinds of hadronic currents

vector currents $J^P = 1^-$

axial vector currents $J^P = 0^-, 1^+,$

where J^P is the spin parity of the hadronic final state. Due to the conservation of the vector current (CVC), no scalar final states occur in the vector part.

a) Vector Current

The vector current with $J^P = 1^-$ leads to the prediction of the decay

$$\tau \rightarrow \nu \rho .$$

Assuming CVC the weak ρ coupling is inferred from the known $\gamma\rho$ coupling

The relative width of the leptonic and the ρ decay is then given by /14/

$$(\Gamma(\tau \rightarrow \nu\rho))/(\Gamma(\tau \rightarrow \nu\nu e)) = 3\pi \cos^2\theta_c (1 - (M_\rho/M_\tau)^2)^2 (1+2(M_\rho/M_\tau)^2)(M_\rho/M_\tau)^2. \quad (23)$$

With $BR(\tau \rightarrow e\nu\nu) = 16.8\ \%$, $M_\rho = .77\ GeV/c^2$ and $M_\tau = 1.8\ GeV/c^2$ this yields

$BR(\tau \rightarrow \rho\nu) = 25.3\ \%$ Theory /14/.

DASP has studied this decay channel in the reaction

$$e^+ e^- \rightarrow \pi^\pm + 1 \text{ track} + 2 \text{ photons}, \quad (24)$$

where the π was measured in one of the spectrometers and the other particles were seen in the inner detector /40/. Events are retained if a π^0 can be fitted to the photons. Fig. 21 shows the mass distribution of the $\pi^\pm\pi^0$ system and its momentum distribution for events from the ρ band ($.5 < M_{\pi^\pm\pi^0} < 1.0$ GeV). Since about 40 % of the events contain an electron (hatched in Fig. 21), multihadron events cannot explain the data. On the other hand, the $(\tau \rightarrow \nu\rho)$ decay in

$$e^+ e^- \rightarrow \tau\,\tau \begin{cases} \rightarrow 1 \text{ track} \\ \rightarrow \nu\rho \end{cases} \quad (25)$$

does explain both the electrons and the $\pi^{\pm}\pi^{0}$ momentum distribution. From events above 1 GeV/c ρ momentum the preliminary value of

$$BR(\tau \to \nu\rho) = (24 \pm 9)\ \% \qquad \text{DASP /40/}$$

is obtained, in good agreement with theory.

b) Axial Vector Current

Since the axial vector current is not conserved, its divergence can also contribute to the hadronic current. Therefore, $J^P = 0^-$ and 1^+ final states are allowed. Consequently, the τ will decay into $\nu\pi$ and νA_1 (if the A_1 exists) or other 0^- and 1^+ states.

($\tau \to \nu\pi$) Decay

This decay plays a central rôle in the discussion of the weak current involved in τ decay since it constitutes the "inversion" of the μ decay and can therefore unambiguously be predicted from the pion coupling constant f_π (Fig. 20c,d).

The relative width is given as /14/

$$\Gamma(\tau \to \pi\nu) \,/\, \Gamma(\tau \to e\nu\nu) = 12\pi^2 \, f_\pi^2 \, \cos^2\theta_c \, / M_\tau^2 \qquad (26)$$

With $BR(\tau \to e\nu\nu) = 16.8\ \%$, $f_\pi = .129$ GeV/c^2 and $M_\tau = 1.8$ GeV/c^2 this yields

$$BR(\tau \to \pi\nu) = 9.5\ \% \qquad \text{Theory /14/.}$$

The PLUTO group studied inclusive pion production /41/ from the reaction:

$$e^+ e^- \to \tau\,\tau \;\begin{cases} \to \pi\nu \\ \to \text{1 prong + no photons.} \end{cases}$$

32 events of the signal class

$$e^+ e^- \to \text{hadron + 1 charged track + no photon}$$

were seen in the 4 to 5 GeV energy range. On the other hand, only 8.9 ±1.0 events were expected from hadron misidentification, $\tau \to \rho\nu$ decay and hadronic sources. Fig. 22 shows the momentum spectrum of hadrons at 5 GeV compared to muons with the same kinematical cuts. The hadron spectrum is indeed shifted to larger momenta, as expected from a twobody decay. The PLUTO group obtains a branching ratio of

$$BR(\tau \to \pi\nu) = (9.0 \pm 2.9)\ \% \qquad \text{PLUTO /41/}$$

with an additional systematic uncertainty of 2.5 %. Going along very similar lines, the SLAC-LBL group found a branching ratio of

$$BR(\tau \to \pi\nu) = (9.3 \pm 3.9)\ \% \qquad \text{SLAC-LBL /12/ .}$$

DELCO studied /12/ events of the type

$$e^+ e^- \to e^{\pm} + \text{hadron} + \text{no photons.}$$

They observed 10.7 events after background subtraction. 11.8 events are expected, out of which only 2.8 events are due to other sources than π decay (mainly $\tau \to \rho\nu$). The resulting branching ratio is

$$BR(\tau \to \pi\nu) = (8.3 \pm 3.0)\ \% \qquad \text{DELCO /12/.}$$

$(\tau \to A_1\nu)$ Decay

This second candidate for an axial vector piece in the hadronic current can only be calculated if one introduces further assumptions about the relative size of the axial and vector current (Weinberg sum rules). The width of

$$\tau \to A_1\ \nu$$

relative to the leptonic width is then given by

$$\Gamma(\tau \to A_1\nu)\ /(\Gamma(\tau \to e\nu\nu) = 3/4\ \pi\ \cos^2\theta_c (1 - (M_{A_1}/M_\tau)^2)^2 \cdot \cdot\ (1 + 2(M_{A_1}/M_\tau)^2)\ (M_{A_1}/M_\tau)^2 \qquad (27)$$

+) Conversely a measurement of $BR(\tau \to \nu A_1)$ allows to determine the coupling constant f_{A_1} and to check Weinbergs rules.

With $BR(\tau \to e\nu\nu) = 16.8\ \%$, $M_\tau = 1.8\ GeV/c^2$ and $M_{A_1} = 1.07\ GeV/c^2$ this yields

$$BR(\tau \to A_1\nu) = 8.1\ \% \qquad \text{Theory /14/.}$$

The PLUTO collaboration has searched /37,39,42/ for events from the reaction

$$e^+ e^- \to \tau\,\tau \begin{cases} \to e\nu\nu, \mu\nu\nu \\ \to \pi^{\pm} + \pi + \pi \end{cases} \tag{28}$$

in the energy range from 4 to 5 GeV. They found 54 events of the type

$$e^+ e^- \to \begin{matrix} e \\ \mu \end{matrix} + \pi^{\pm} \pi^+ \pi^- \tag{29}$$

which were kinematically consistent with reaction (28). Fig. 23 shows the mass distribution of the two possible $\pi^+\pi^-$ combinations of each event. The ρ signal sticks out most clearly in the high mass combination, which is hatched in the histogram. 40 events are retained with at least one $\pi^+\pi^-$ mass in a ρ band of $.68 < M_{\pi\pi} < .86\ GeV/c^2$. There is an estimated background of 8.5 events in the ρ band mainly from purely hadronic 4 prong events where one hadron misidentified as electron or muon. The remaining 14 (hatched) events outside the ρ band do not exceed significantly the background estimate of 9.5 events. The PLUTO group therefore concludes that the whole signal is due to the decay

$$\tau \to \rho^0 \pi \nu$$

Assuming I = 1 for the $\rho\pi$ system one can determine a branching ratio of

$$BR(\tau \to \rho\pi\nu) = (10.4 \pm 2.4)\ \% \qquad \text{PLUTO /37,42/}$$

with an additional systematic uncertainty of 2 %.

The existence of a $\rho\pi$ final state with negative G-parity in itself proves that an axial piece is present in the hadronic weak current in τ decays, provided only first class currents are present.[+] To get a statement independent of the latter assumption, the spin parity of the $\rho\pi$ system was studied. The density distribution in a 3-dimensional Dalitz plot of the masses of the two $\pi^+\pi^-$ combinations and the $\rho\pi$ system was investigated. Only the $J^P = 1^+$ s-wave and the

[+] By definition of first class currents /50/.

$J^P = 2^-$ p-wave gave an acceptable description of the data. Fig. 24a shows the mass distribution of the $\rho\pi$ system together with the expectation from a Monte-Carlo calculation for different partial waves. The p and d waves give a very bad account of the data. Only the

$$J^P = 1^+ \text{ s-wave}$$

is acceptable. This proves again the existence of an axial part in the hadronic current. In particular, there are no indications for a 1^- s-wave from second class axial currents.

The $\rho\pi$ mass distribution is much better described by assuming a resonance of $M = 1$ GeV and $\Gamma = .475$ GeV in the 1^+ s-wave (Fig. 24b). This indicates that the observed decay may indeed be due to

$$\tau \rightarrow A_1 \nu \rightarrow \rho \pi \nu \, . \tag{30}$$

The evidence is not compelling, however.

The SLAC-LBL group has studied the reaction

$$e^+ e^- \rightarrow \mu^{\pm} + \pi^{\mp} \pi^+ \pi^- + \geq 0 \text{ photons} \, . \tag{31}$$

From the momentum distribution of the muon and the 3π system they show that the events originate from a process of type (28) with one τ decaying into pions

$$\tau^- \rightarrow \nu_\tau \pi^- \pi^+ \pi^- + n \pi^0 \, . \tag{32}$$

The three pion-mass distributions are given in Fig. 25 for different numbers of observed photons. The clear enhancement around a 3π mass of 1.1 GeV/c^2 contains 42 events ($.95 \rightarrow M_{3\pi} < 1.25$ GeV; $n\gamma \leq 2$). Only few events are associated with kaons, proving that the signal does not originate predominantly from charm. The branching ratio is

$$BR(\tau^- \rightarrow \nu_\tau + \pi^- \pi^+ \pi^- + n \pi^0) = (16 \pm 6) \% \, .$$

From a comparison of 0 γ and 1,2 γ data the purely charged decay mode can be estimated

$$BR(\tau^- \to \nu_\tau + \pi^- \pi^+ \pi^-) = (6 \pm 4.5)\ \%$$

in good agreement with the PLUTO result. An acceptable description of the 3π mass distribution is again obtained from a fit assuming $(\tau \to A_1 \nu)$ decay with $M_{A_1} = 1.1\ \mathrm{GeV/c^2}$ and a width $\Gamma_{A_1} = 200\ \mathrm{MeV/c^2}$.

c. Strangeness

Since the τ mass is below the charm threshold, decays involving strange particles should be suppressed by $tg^2\theta_c \approx 5\ \%$. The DASP group measured /27/ the ratio of kaon to pion production in two-prong events with one electron, which are dominated by τ production. Their result

$$(\sigma(e^+e^- \to e + K + \geq 0\ \gamma's))/(\sigma(e^+e^- \to e + \pi + \geq 0\gamma's)) = (7 \pm 6)\ \%$$ DASP /27/

is in accordance with theory.

d. Hadron Continuum

The remaining part of the semihadronic decay

$$\tau \to \nu_\tau + \text{hadron continuum}$$

can be calculated from the quark model. Using CVC, the quark model with colour and assuming that the vector part is equal to the axial part one obtains the value /14/ given in Table 2. Only a small fraction of the hadronic final states is expected to contain a single charged particle /44/. Therefore, a rough test of this number can be obtained from a comparison with experimental results on multiprong final states:

$BR(\tau \to \nu_\tau + \geq 3$ prongs)	=	(30 ±10) %	PLUTO /6/
		(35 ±11) %	DASP /27/
		(32 ± 5) %	DELCO /33/

In fact the experimental results agree quite well with the theoretical prediction of multiprong final states, which is given by the sum of the continuum and half the A_1 branching ratio.

4. Rare Decay Modes

Several decays, which are not allowed by the standard model, have been searched for. None of them has been detected. A summary of upper limits is given in Table 5.

5. Associated Neutrino

So far, data have been discussed in the framework of the "standard model", where the τ has its own neutrino ν_τ. However, many other models have been put forward, which very much resemble the standard model in their experimental consequences. Without going into the details of any specific model /45/, I will only discuss the phenomenological question, whether a distinct τ neutrino exists or whether it is identical to one of the known neutrinos.

Minimal Assumptions

The question has been discussed whether minimal assumptions with just one additional charged lepton $L^{\pm}$ (no neutral partner) could explain the heavy lepton data /46/. Due to lepton number mixing, this model leads to neutral current contributions with branching ratios:

$$BR(L \to \begin{matrix} e \\ \mu \end{matrix} + \text{hadrons}) \quad \sim .30$$

$$BR(L \to 3 \text{ charged leptons}) \quad \sim .05$$

which is excluded by the data of Table 5.

Ortholeptons and Paraleptons

Llewellyn Smith has proposed a classification for models of new leptons with old lepton numbers /47/. Ortholeptons are particles with the quantum number of an old lepton of the same charge, whereas paraleptons are those with the quantum number of the oppositely charged electron or muon.

For paraleptons (with V ±A and massless neutrino) there is a difference of a factor of 2 in the statistical weight of muon and electron decay. Consequently for the electron type lepton $E^{\pm}$

$$BR(E^- \rightarrow \bar{\nu}_e e^- \bar{\nu}_e)/BR(E^- \rightarrow \bar{\nu}_e \mu^- \bar{\nu}_\mu) = 2 \qquad (32)$$

whereas for the muon type lepton this ratio is 0.5. This is excluded by the experimental data of section V.2.

The simplest case of an ortholepton, where the τ would be an excited e or μ and would decay electromagnetically, is excluded by the data of Table 5. This does, however, not exclude ortholeptons with only weak coupling /48/. For them, a neutral current coupling can occur and - like above - produce semihadronic and three charged lepton decays. Since the strength of this coupling depends on the model, no general conclusion can be drawn from Table 5. We can only exclude ortholeptons with conventional coupling strength.

The muonic case, however, can be ruled out completely, since the lower limit of 13 % of the conventional strength deduced from the lifetime limit (section V.1) conflicts with an upper limit of 2.5 % from neutrino experiments /49/.

Consequently, the only possibility left beside the standard model is an electronic ortholepton with less than the conventional coupling strength.

VI. SUMMARY

Since the first result about $e\mu$ final states at SLAC in 1975 the evidence for the existence of a new heavy lepton τ has been increased steadily. Today, the τ is undoubtedly established as a new spin 1/2 particle of mass

$$M_\tau = 1.782 \begin{matrix} + .002 \\ - .017 \end{matrix} \text{ GeV}/c^2.$$

The data summarized in Table 6 agree with the expectation of the standard model of a sequential lepton, which couples to the conventional weak interaction with its own spin 1/2 neutrino.

ACKNOWLEDGEMENT:

I am deeply indebted to my colleagues at DESY in particular in the PLUTO collaboration who helped me in the preparation of this report.

Table 1 Predictions for $R = \sigma_{had}/\sigma_{\mu\mu}$

	without colour	with colour
3 quarks (u, d, s)	2/3	2
4 quarks (u, d, s, c)	1 1/9	3 1/3

Table 2 Predicted branching ratios for a sequential heavy lepton of mass $M_\tau = 1.8$ GeV/c^2

decay mode	charged particles	$BR(\tau^- \to \nu_\tau + \ldots)$
$\tau \to \nu_\tau\ e^-\ \bar{\nu}_e$	1	16.8 %
$\nu_\tau\ \mu^-\ \bar{\nu}_\mu$	1	16.4 %
$\nu_\tau\ \pi^-$	1	9.5 %
$\nu_\tau\ K^-$	1	0.5 %
$\nu_\tau\ \rho^-$	1	25.3 %
$\nu_\tau\ K^{*-}$	1	1.3 %
$\nu_\tau\ A_1^-$	1.3	8.1 %
$\nu_\tau\ Q^-$	1.3	0.3 %
ν_τ (hadron continuum)	1.3.5	21.8 %

Table 3 Summary of μe events /11/ $e^+e^- \to \mu^\pm e^\mp$ + missing energy

collaboration	momentum cuts (GeV/c)	events	background	reference
SLAC-LBL	$p_e > .65$ $p_\mu > .65$	190	46	5
PLUTO	$p_e > .25$ $p_\mu > 1.0$	23	≤ 2	6
Lead-Glass-Wall	$p_e > .4$ $p_\mu > .65$	22	.4	34
DASP	$p_e > .2$ $p_\mu > .7$	13	1.2 ±.4	27

Table 4 Summary of leptonic branching ratios. For the average, $B_e = B_\mu$ is assumed and the statistical (first) and systematic (second) errors are added quadratically.

collaboration	$B_e = BR(\tau \to e\nu\nu)$ [%] $B_\mu = BR(\tau \to \mu\nu\nu)$	reference
SLAC-LBL	$B_e = B_\mu = 18.6 \pm 1.0 \pm 2.8$	29
	$B_\mu = 17.5 \pm 2.7 \pm 3.0$	29
PLUTO	$B_\mu = 15.0 \pm 3.0$	6,30
	$B_e = 16.5 \pm 5.6$	6,30
Lead-Glass-Wall	$B_e = B_\mu = 22.4 \pm 3.2 \pm 4.4$	34
Ironball	$B_\mu = 22\ ^{+7}_{-8}$	11
MPPS	$B_\mu = 20 \pm 10$	11
DASP	$B_e = B_\mu = 18.2 \pm 2.8$	27
DELCO	$B_e = 16.0 \pm 1.3$	33
World Average	$B_e = B_\mu = 16.7 \pm 1.0$	

Table 5 Upper limits for the branching ratios into some potential decay modes

potential decay mode	upper limit %	conf. level %	experiment	reference
$\tau^- \rightarrow$ 1 charged lepton + $\geq$1 charged particle	4	90	PLUTO	6
$\tau^- \rightarrow$ 3 charged particles	1	95	PLUTO	10
$\tau^- \rightarrow$ 3 charged leptons	0.6	90	SLAC-LBL	11
$\tau^- \rightarrow$ 1 charged lepton + photons	12	90	PLUTO	6
$\tau^- \rightarrow e^-$ + photons	2.6	90	SLAC-LBL	11
$\tau^- \rightarrow \mu^-$ + photons	1.3	90	SLAC-LBL	11

Table 6 Summary of τ parameters. World averages or best values are given, for details compare the sections referred to.

parameter	units	prediction	exp. value	experiments	section
mass	GeV/c^2	-	$1.782\ ^{+.002}_{-.007}$	PLUTO, SLAC-LBL, DASP, DESY-Heidelberg, DELCO	IV.2
neutrino mass	MeV/c^2	0	<250	SLAC-LBL, PLUTO, DELCO	V.5
spin		1/2	1/2	PLUTO, DASP, DELCO	V.2
lifetime	10^{-13}s	2.8	< 35	PLUTO, SLAC-LBL	V.1
Michel parameter ρ		.64	.66 ± .13	DELCO	V.2
leptonic branching ratios					
$B_e : \tau^- \to \nu_\tau e^- \bar{\nu}_e$	%	16.8	16.7 ±1.0	SLAC-LBL, PLUTO, Lead-Glass-Wall, Ironball, MPPS, DASP. DELCO	V.2
$B_\mu : \tau^- \to \nu_\tau \mu^- \bar{\nu}_\mu$	%	16.4			
B_μ/B_e		.98	.99 ± .20	SLAC-LBL, PLUTO, DASP	V.2
semihadronic BR					
$\tau^- \to \nu_\tau \pi^-$	%	9.5	8.8 ±2.0	PLUTO, SLAC-LBL, DELCO	V.3.b
$\tau^- \to \nu_\tau \rho^-$	%	25.3	24 +9	DASP	V.3.a
$\tau^- \to \nu_\tau A_1^-$	%	8.1	10.4 ±2.4	PLUTO, SLAC-LBL	V.3.b
$\tau^- \to \nu_\tau$ + ≥3 prongs	%	~26	32 ±4	PLUTO, DASP, DELCO	V.3.d
$\tau^- \to K^- .../\tau^- \to \pi^- ...$		.05	.07 ± .06	DASP	V.3.c

REFERENCES

1. S. Weinberg; Phys. Rev. Lett. 19, 1264 (1967)
   A. Salem, Proc. 8th Nobel Symposium, Stockholm 1968

2. S. L. Glashow, J. Iliopoulos, L. Maiani, Phys. Rev. D2, 1285 (1970)

3. J. J. Aubert et al., Phys. Rev. Lett. 33, 1404 (1974)
   J.-E. Augustin et al., Phys. Rev. Lett. 33, 1406 (1974)

4. S. L. Adler, Phys. Rev. 177, 2426 (1969)
   J. S. Bell, R. Jackiw, Nuovo Cim., 51, 47 (1969)
   C. Bouchiat, J. Iliopoulos, Ph. Meyer, Phys. Lett. 38B, 519 (1972)
   D. J. Gross, R. Jackiw, Phys. Rev. D6, 477 (1972)

5. M.L. Perl et al., Phys. Rev. Lett. 35, 1489 (1975)
   M.L. Perl et al., Phys. Rev. Lett. 38, 117 (1976)

6. PLUTO Coll., J. Burmester et al., Phys. Lett. 68B, 297 (1977)
   PLUTO Coll., J. Burmester et al., Phys. Lett. 68B, 301 (1977)

7. S.W. Herb et al., Phys. Rev. Lett. 39, 252 (1977)
   W.R. Innes et al., Phys. Rev. Lett. 39, 1240 (1977)

8. PLUTO Coll., Ch. Berger et al., Phys. Lett. 76B, 243 (1978)
   C.W. Darden et al., Phys. Lett. 76B, 247 (1978)

9. M.L. Perl, P. Rapidis, SLAC-PUB-1496 (1974) with further references.

10. G. Flügge, Proc. of the Vth Int. Conf. on Experimental Meson Spectroscopy, North Eastern Univ., Boston (April 1977) and DESY 77/35 (1977)

11. M.L. Perl, Proc. of the 1977 Int. Symp. on Lepton and Photon Interactions at High Energies, Hamburg (August 1977)
    M.L. Perl, Proc. of the XII Rencontre de Moriond, Flaine (March 1977) and SLAC-PUB-1923 (April 1977)

12. G.J. Feldman, SLAC-PUB-2138 (June 1978)

13. M. Bernardini et al., Nuovo Cimento 17, 383 (1973)
S. Orito et al., Phys. Lett. 48B, 165 (1976)

14. Y.S. Tsai, Phys. Rev. D4, 2821 (1971)
H.B. Thacker, J.J. Sakurai, Phys. Lett. 36B, 103 (1971)
J.D. Bjorken, C.H. Llewellyn-Smith, Phys. Rev. D7, 887 (1973)

15. G. Goldhaber et al., Phys. Rev. Lett. 37, 255 (1976)
I. Peruzzi et al., Phys. Rev. Lett. 37, 569 (1976)
PLUTO Coll., J. Burmester et al., Phys. Lett. 64B, 369 (1976)
DASP Coll., W. Braunschweig et al., Phys. Lett. 63B, 471 (1976)

16. DASP Coll., B. Brandelik et al., Phys. Lett. 70B, 387 (1977)

17. L. Criegee et al., Proc. 1973 Int. Conf. on Instrumentation for HEP, Frascati (1973)
PLUTO Coll., J. Burmester et al., Phys. Lett. 64B, 369 (1976)

18. G.J. Feldman, M.L. Perl, Phys. Reports 19C, 234 (1975)
J.-E. Augustin et al., Phys. Rev. Letters 34, 233 (1975)

19. M. Cavalli-Sforza et al., Phys. Rev. Lett. 36, 558 (1976)

20. H.F.W. Sadrozinski, Proc. of the 1977 Int. Symp. on Lepton and Photon Interactions at High Energies, Hamburg (August 1977)

21. J.M. Feller et al., IEEE Trans. on Nucl. Sci. NS-25, 304 (1978)

22. DASP Coll., W. Braunschweig et al., Phys. Lett. 63B, 417 (1976)
DASP Coll., W. Braunschweig et al., Phys. Lett. 67B, 243 (1977)

23. W. Bacino et al., Phys. Rev. Lett. 40, 671 (1978)

24. W. Bartel et al., Phys. Lett. 66B, 483 (1976)

25. J. Siegrist et al., Phys. Rev. Lett. 36, 700 (1976)

26. PLUTO Coll., J. Burmester et al., Phys. Lett. 66B, 395 (1977)
A. Bäcker, Thesis, Siegen (1977), Internal Report DESY F33-77/03 (unpubl.)

27. DASP Coll., R. Brandelik et al., Phys. Lett. 70 B, 125 (1977)
DASP Coll., R. Brandelik et al., Phys. Lett. 73B, 109 (1978)

28. T.W. Appelquist, H. Georgi, Phys. Rev. D8, 4000 (1973)
A. Zee, Phys. Rev. D8, 4038 (1973)

29. G.J. Feldman et al., Phys. Lett. 63B, 466 (1976)
M.L. Perl et al., Phys. Lett. 70B 487 (1977)

30. M. Rößler, Thesis, Hamburg (1978), Internal Report F14-78/01 (unpubl.)

31. F. Gutbrod, Z.J. Rek, DESY 77/45 (1977)

32. PLUTO Coll., J. Burmester et al., Phys. Lett. 68B, 283 (1977)

33. W. Bacino et al., SLAC-PUB-2113 (1978)

34. A. Barbaro-Galtieri et al., Phys. Rev. Lett. 39, 1058 (1977)

35. W. Bartel et al., DESY 78/24 (1978) submitted to Phys. Lett.

36. K. Fujikawa, N. Kawamoto, Phys. Rev. D14, 59 (1976) with further references.

37. U. Timm, invited talk at the 3rd Int. Conf. on New Results in High Energy Phys., Nashville (1978) and DESY 78/25 (1978)

J. Bürger, invited talk at the XIII Rencontre de Moriond, Les Arcs (1978) and Univ. Siegen SI 78-10 (1978)

38. F.B. Heile et al., SLAC-PUB-2059 (1977) to be published in Nucl. Phys. B

39. G. Knies, Proc. of the 1977 Int. Symp. on Lepton and Photon Interactions at High Energies, Hamburg (August 1977)

40. B.H. Wiik, G. Wolf, DESY 78/23 (1978)

41. PLUTO Coll., G. Alexander et al., DESY 78/30 (1978) submitted to Phys. Lett.

42. PLUTO Coll., G. Alexander et al., Phys. Lett. 73B, 99 (1978)
W. Wagner, Thesis, Aachen (1978)

43. J.A. Jaros et al., Phys. Rev. Lett. 40, 1120 (1978)

44. F.J. Gilman, D.H. Miller, Phys. Rev. D17, 1846 (1978)

45. T.F. Walsh, Proc. of the 1977 Int. Symp. on Lepton and Photon Interactions at High Energies, Hamburg (August 1977)

46. G. Altarelli, N. Cabibbo, L. Maiani, R. Petronzio, Phys. Lett. 67B, 463 (1977)
D. Horn, D.D. Ross, Phys. Lett. 67B, 460 (1977)

47. C.H. Llewellyn-Smith,
Proc. Royal Soc. A355, 585 (1977)

J.D. Bjorken, C.H. Llewellyn-Smith, Phys. Rev. D7, 887 (1973)

48. F.E. Low, Phys. Rev. Lett. 14, 238 (1965)

49. M. Murtagh, K. Schultze, Proc. of the 1977 Int. Symp. on Lepton and Photon Interactions at High Energies, Hamburg (August 1977)
A.M. Cnops et al., Phys. Rev. Lett. 40, 144 (1978)

50. S. Weinberg; Phys. Rev. 112, 1375 (1958)

Figure Captions

Fig. 1 PLUTO detector, viewed along the beam.

Fig. 2 SLAC-LBL detector, exploded view.

Fig. 3 DASP detector, blow up picture. M = magnet, DK = proportional or spark chamber, F = time-of-flight counters, S = shower counters, R = range counters, Fe = iron, SR = beam pipe.

Fig. 4 DELCO detector, polar and azimuthal projections.

Fig. 5 DESY-Heidelberg detector, viewed along the beam.

Fig. 6 PLUTO: total cross section between 3.5 and 5 GeV center of mass energy in terms of $R = \sigma_{had}/\sigma_{\mu\mu}$.

Fig. 7 MPP S , SLAC-LBL, and PLUTO: inclusive muon production in the 4 to 7 GeV CM energy range. The SLAC-LBL data are scaled to the 1 GeV/c momentum cut using factors of .637, .744, .925 for $s^{1/2} = 4.05$, 4.4, 6.9. This assumes V-A and approximate cancellation of the difference between PLUTO and SLAC-LBL in acoplanarity and missing mass cuts. The MPP S data are for $p_\mu \geq 1.05$ GeV/c, extrapolated to the full solid angle assuming an isotropic distribution of muons. The full curve is a fit to the PLUTO data using the standard model ($m_\tau = 1.9$ GeV).

Fig. 8 DASP: cross section for inclusive electron production in the two-prong class with any number of photons. The solid curves are fits assuming pair production of pointlike particles with spin 0, 1/2 and 1.

Fig. 9 DELCO: inclusive electron production in the twoprong class with any number of photons. The ratio of the electron to μ pair production is plotted versus CM energy. Data are compared with the prediction for spin 0, 1/2 and 1 pair production.

Fig. 10 DESY-Heidelberg: observed cross section for electron and muon two-prong events without photons. The full and dashed curves are fits to the electron and muon data assuming τ pair production.

Fig. 11 PLUTO: example of a μe event.

Fig. 12 SLAC-LBL: observed μe production cross section as a function of CM energy. The full curves are fits for heavy lepton production with M_τ = 1.8 and 2.0 GeV/c^2.

Fig. 13 PLUTO: energy dependence of the μe cross section in comparison to the inclusive twoprong and multiprong data. Cross sections are given for muon momenta > 1 GeV/c. The solid line shows the prediction for a heavy lepton with V-A coupling and M_τ = 1.91 GeV/c^2.

Fig. 14 SLAC-LBL: collinearity distribution of the two leptons in $e\mu$ events at different energies.

Fig. 15 DASP: electron momentum spectrum for events with an electron, a non-showering track and any number of photons. (Above 1 GeV/c momentum also muons have been included with an appropriate weighting.)

Fig. 16 DELCO: electron momentum distribution for twoprong events. Data are compared with the prediction for V-A (solid curve) and V+A (dashed curve) coupling of the τ.

Fig. 17 SLAC-LBL: distribution of the scaled momentum r compared to different hypotheses. The solid curves are for the standard model, V-A coupling, with the neutrino mass indicated in the figure. The dashed curve is for V+A coupling and massless neutrino.

$$r = (p - .65 \text{ GeV/c})/(p_{max} - .65 \text{ GeV/c})$$

Fig. 18 PLUTO: momentum distribution of the muon in inclusive twoprong events for three different energy bins.

Fig. 19 PLUTO: momentum distribution of the muon in inclusive multiprong events at $s^{1/2}$ = 5 GeV.

Fig. 20 Leptonic and semihadronic decays of the heavy lepton τ.

Fig. 21 DASP: ρ decay of the τ.

a) mass distributions for the $\pi^{\pm}\pi^{0}$ system.

b) momentum distribution of the $\pi^{\pm}\pi^{0}$ system in the ρ band.

Fig. 22 PLUTO: π decay of the τ. Momentum distribution of the hadron compared to the muon in twoprong events without photons at 5 GeV CM energy.

Fig. 23 PLUTO: $\rho\pi$ decay of the τ. The squares indicate the background. Mass distribution of the $\pi^{+}\pi^{-}$ system. The shaded area represents the high mass combination.

Fig. 24 PLUTO: $\rho\pi$ decay of the τ. Data corrected for background and acceptance.

a) Mass distribution of the 3π system in the ρ band ($.68 < M_{\pi^+\pi^-} < .86$ GeV/c^2). The curves represent phasespace calculations for different partial waves of the $\rho\pi$ system.

b) The same mass distribution with a fit of a resonant s-wave with M_{A_1} = 1.0 GeV/c^2 and Γ_{A_1} = 475 MeV/c^2.

Fig. 25 SLAC-LBL: 3π decay of the τ. Invariant mass distribution of the 3π system for events with no, one or two, or more than two photons. The distributions are corrected for background from hadron to muon misidentification.

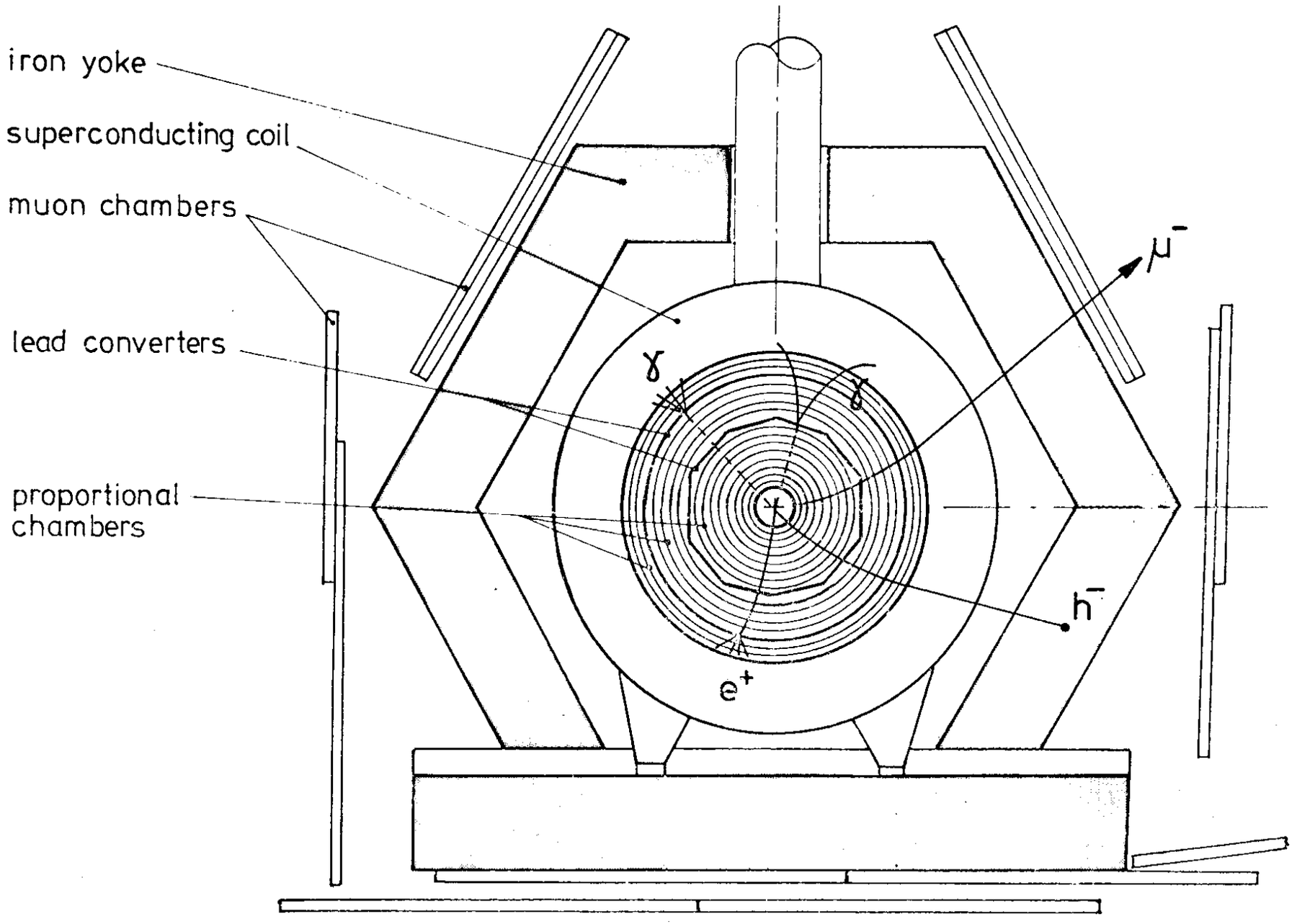
iron yoke
superconducting coil
muon chambers
lead converters
proportional chambers
γ
γ
μ⁻
h⁻
e⁺

FIG.1

25330

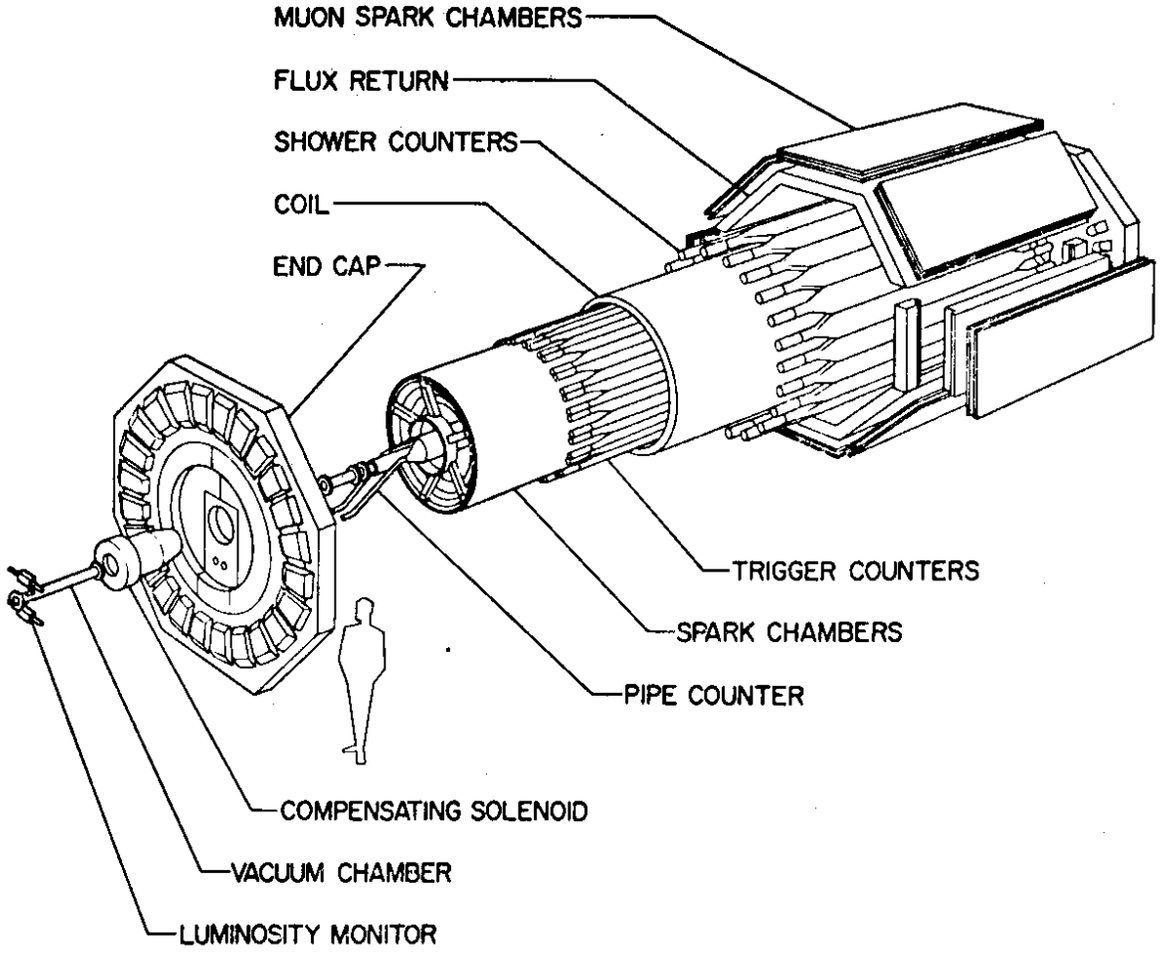
MUON SPARK CHAMBERS
FLUX RETURN
SHOWER COUNTERS
COIL
END CAP
TRIGGER COUNTERS
SPARK CHAMBERS
PIPE COUNTER
COMPENSATING SOLENOID
VACUUM CHAMBER
LUMINOSITY MONITOR

FIG.2

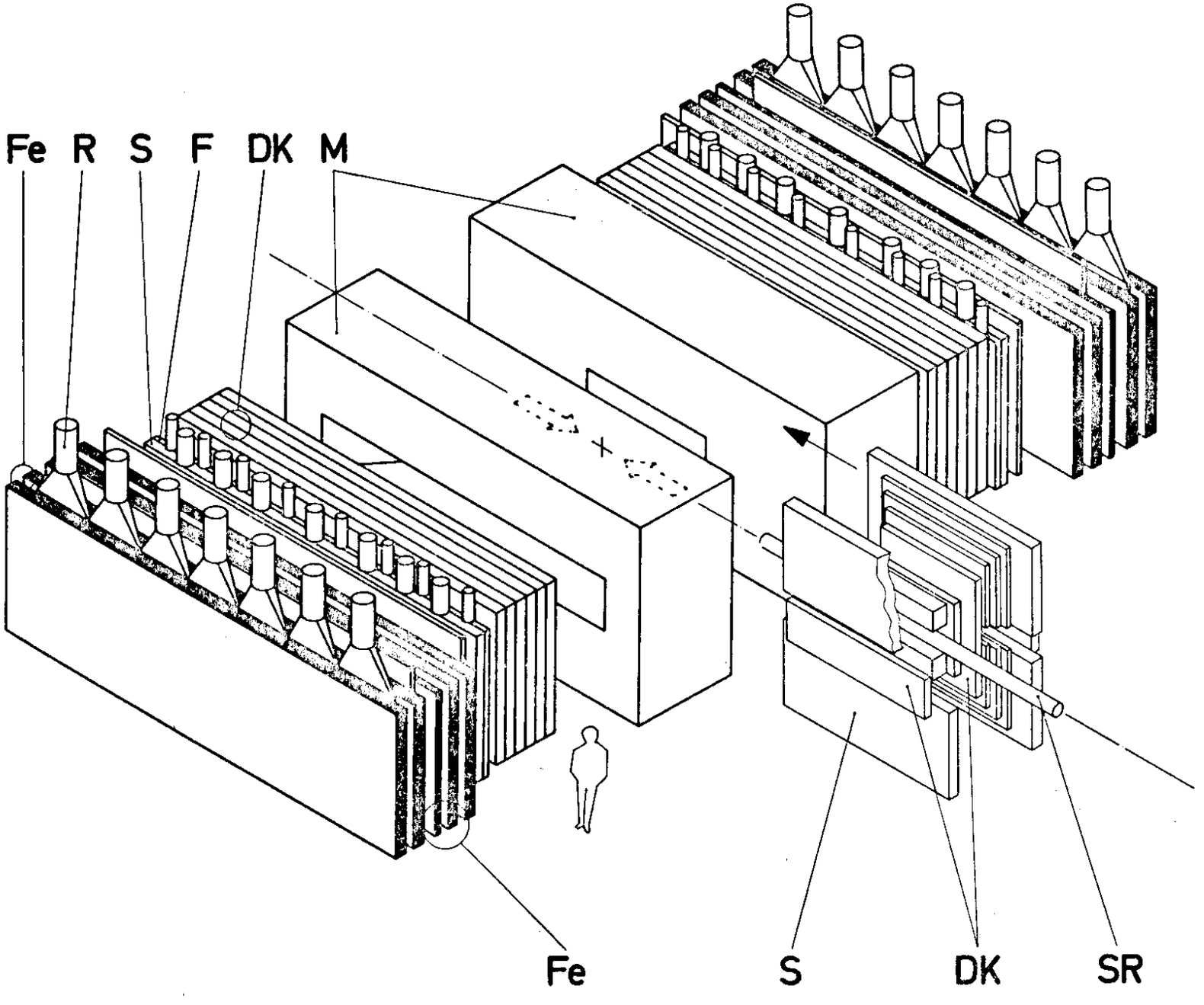

FIG.3

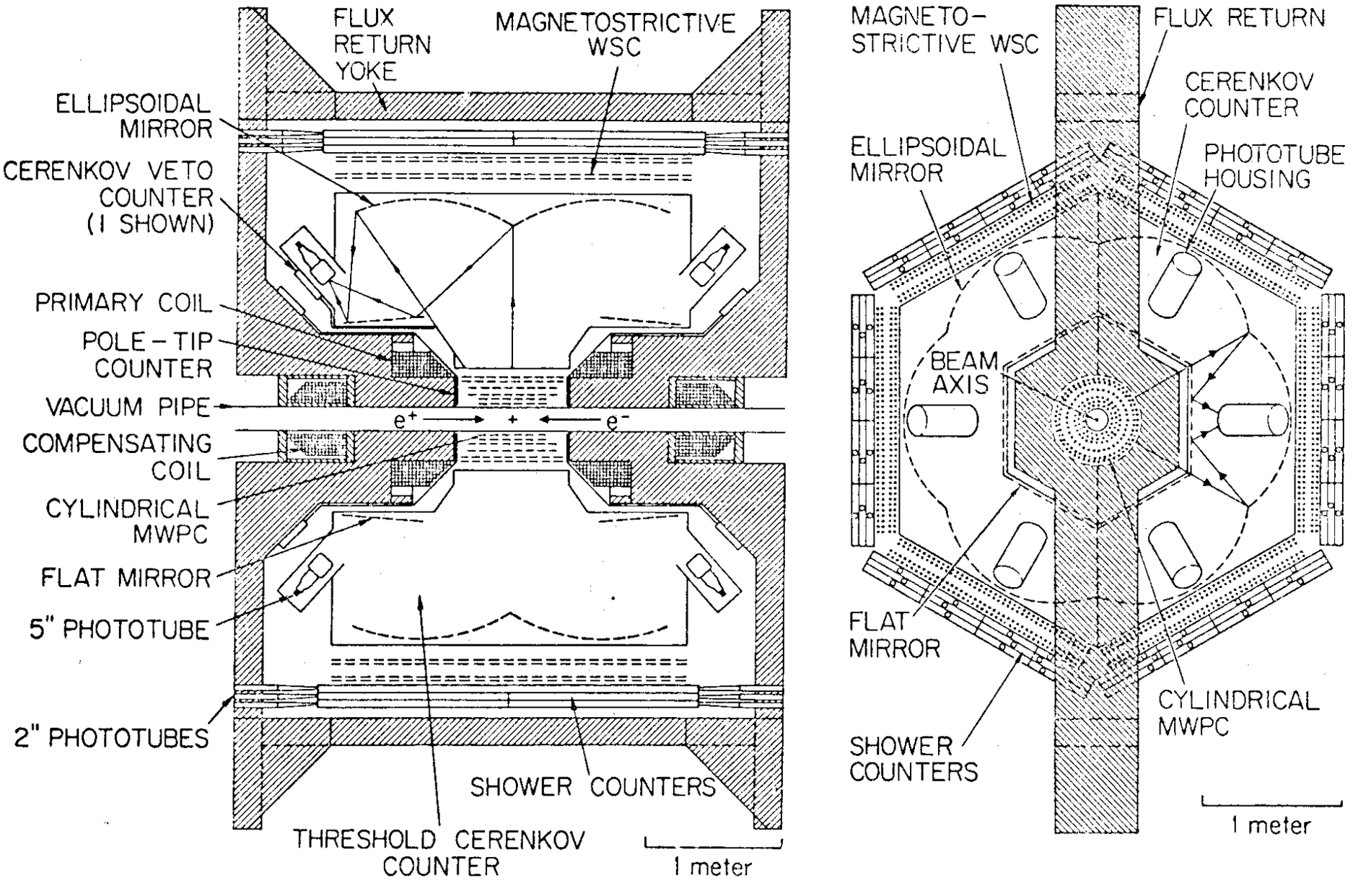
FLUX RETURN YOKE
MAGNETOSTRICTIVE WSC
ELLIPSOIDAL MIRROR
CERENKOV VETO COUNTER (1 SHOWN)
PRIMARY COIL
POLE-TIP COUNTER
VACUUM PIPE
e+
e-
COMPENSATING COIL
CYLINDRICAL MWPC
FLAT MIRROR
5" PHOTOTUBE
2" PHOTOTUBES
SHOWER COUNTERS
THRESHOLD CERENKOV COUNTER
1 meter
MAGNETO-STRICTIVE WSC
FLUX RETURN
CERENKOV COUNTER
ELLIPSOIDAL MIRROR
PHOTOTUBE HOUSING
BEAM AXIS
FLAT MIRROR
CYLINDRICAL MWPC
SHOWER COUNTERS
1 meter

FIG.4

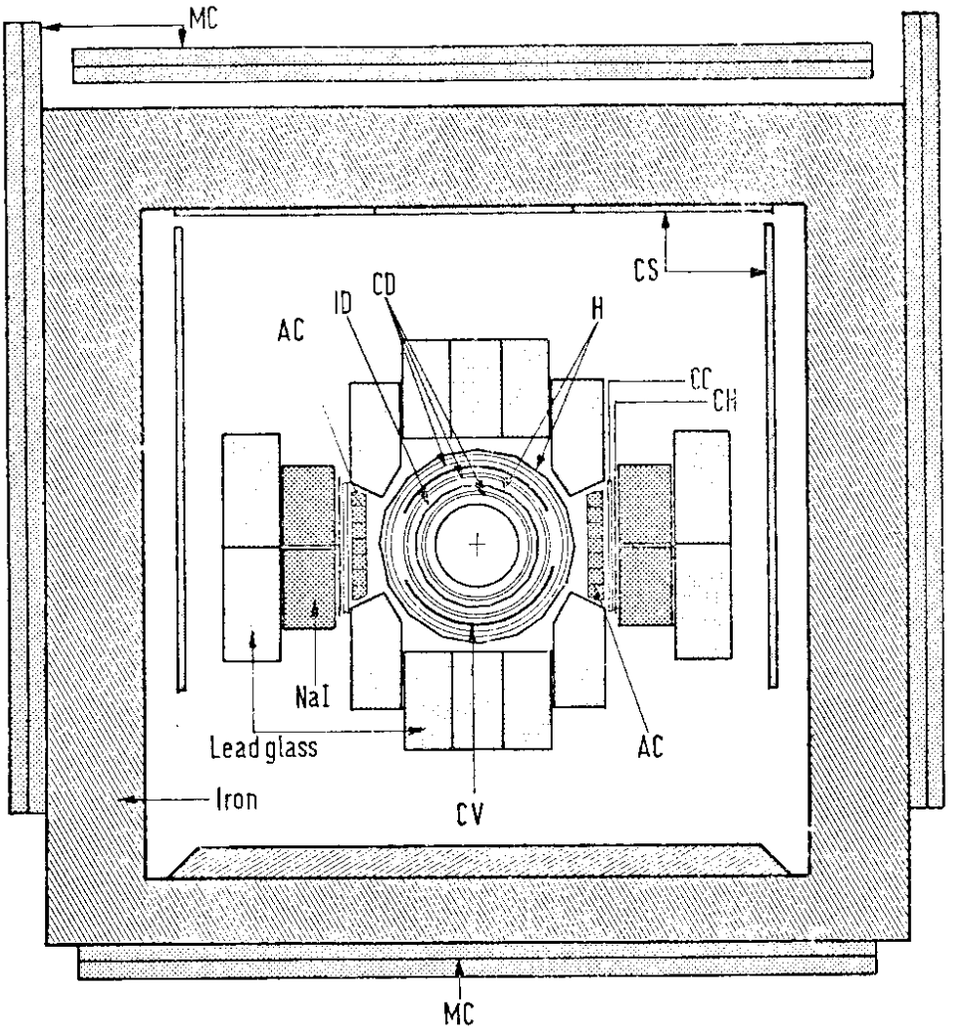

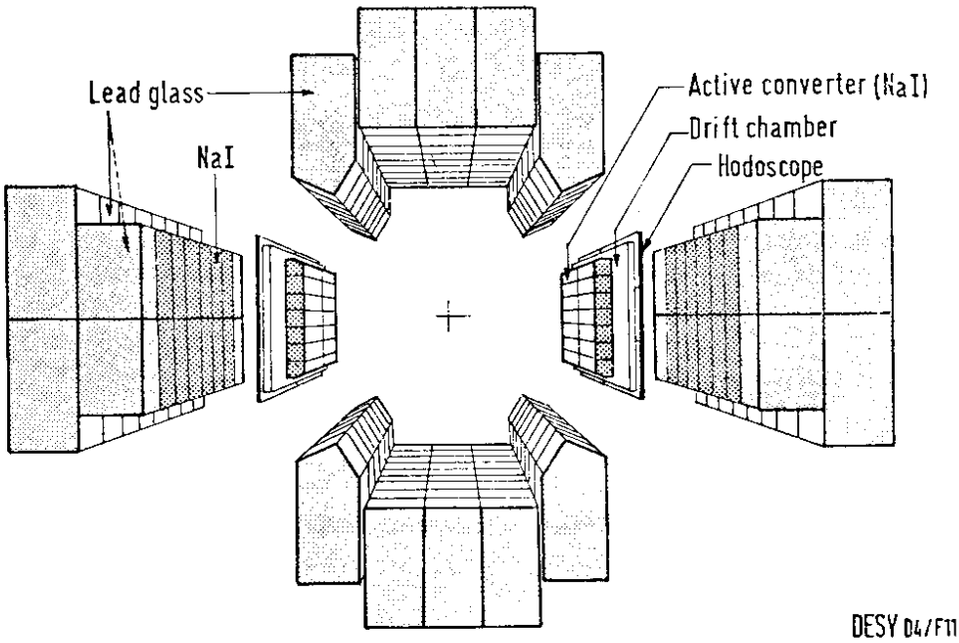

DESY D4/F11-10/77 Knaut

FIG.5

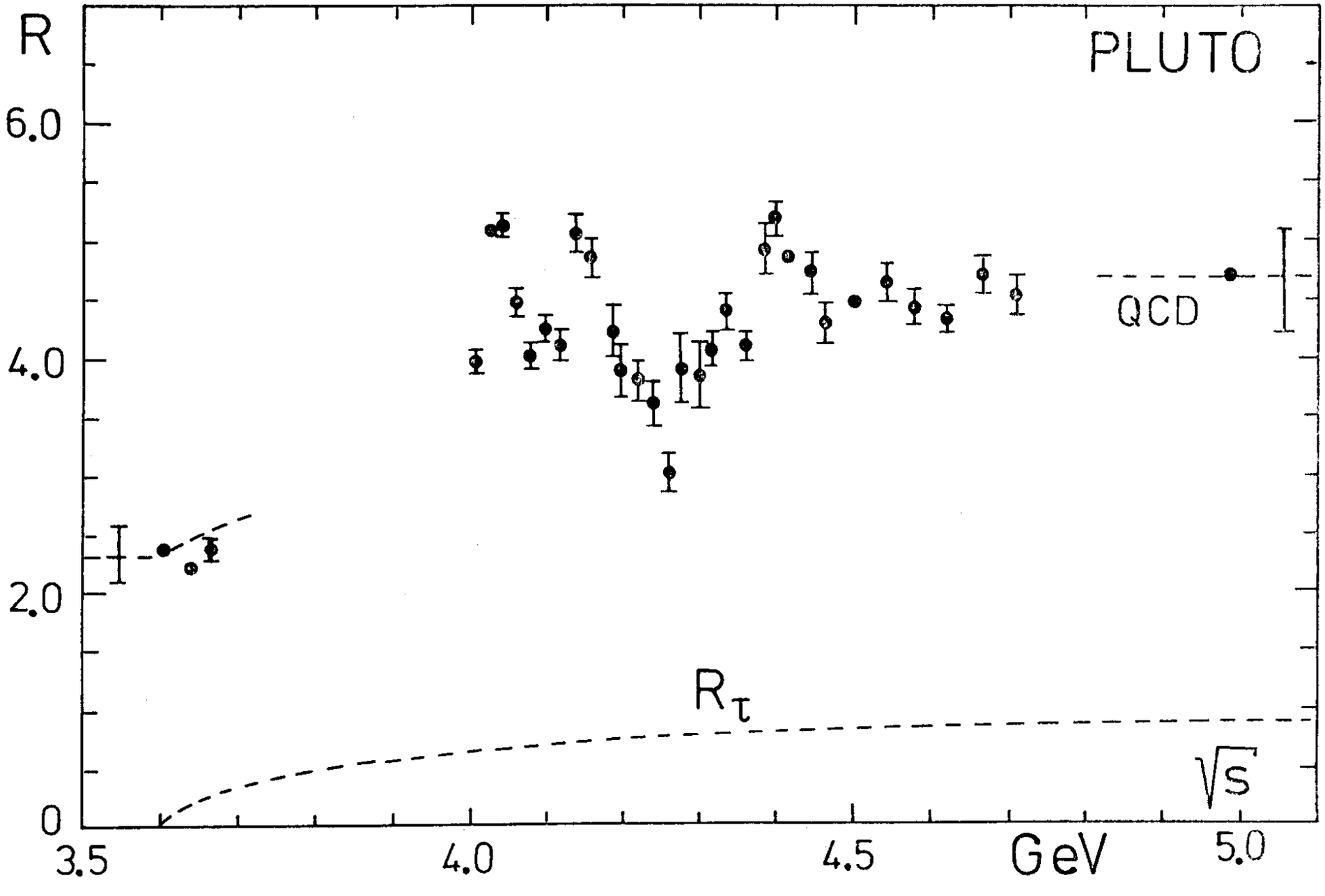

FIG.6

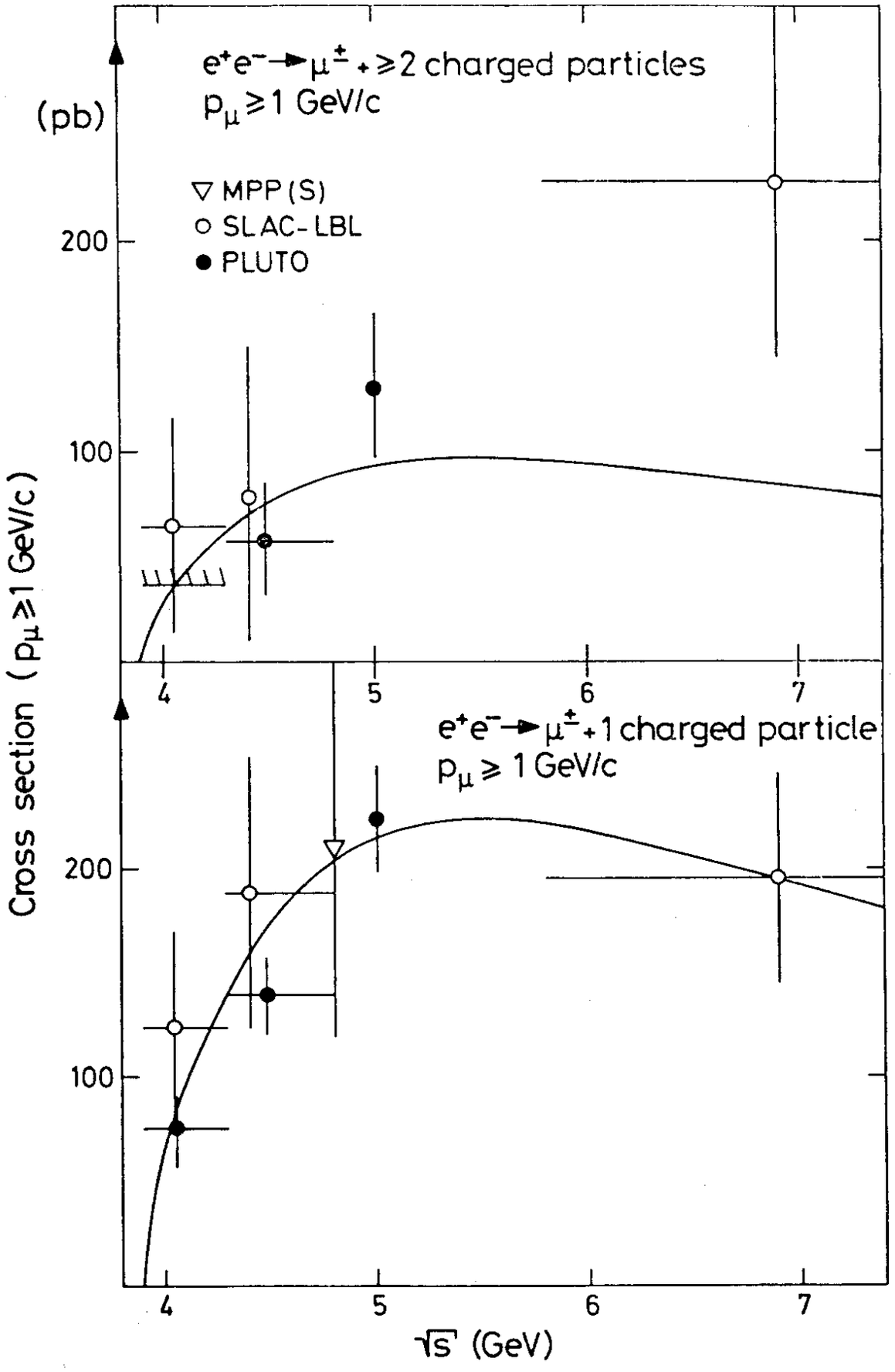
$e^+e^- \rightarrow \mu^\pm + \geq 2$ charged particles
$p_\mu \geq 1$ GeV/c
(pb)
MPP (S)
SLAC-LBL
PLUTO
200
100
4
5
6
7
$e^+e^- \rightarrow \mu^\pm + 1$ charged particle
$p_\mu \geq 1$ GeV/c
200
100
Cross section ($p_\mu \geq 1$ GeV/c)
4
5
6
7
$\sqrt{s}$ (GeV)

FIG.7

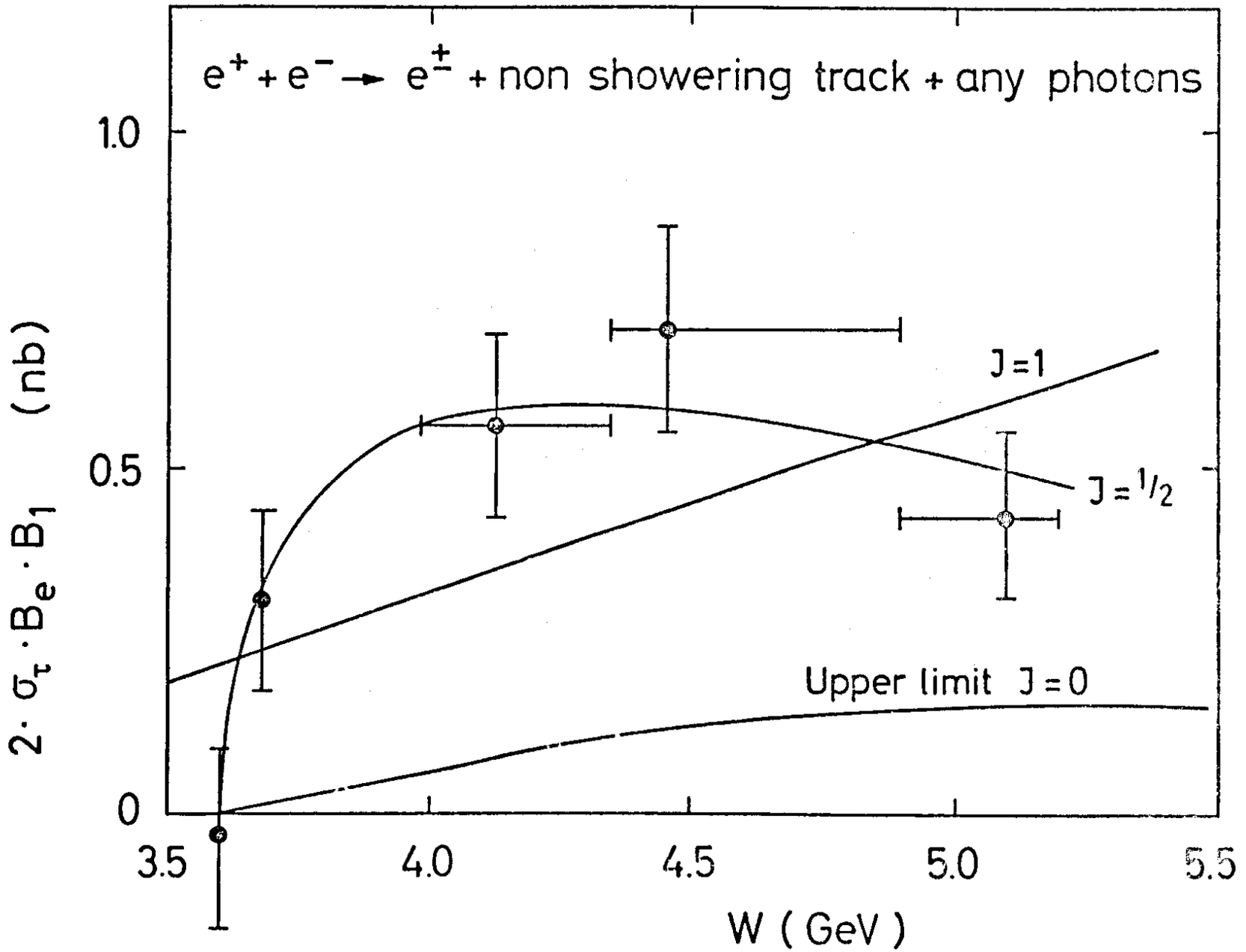
$e^+ + e^- \rightarrow e^{\pm}$ + non showering track + any photons
1.0
0.5
0
$2 \cdot \sigma_\tau \cdot B_e \cdot B_1$ (nb)
J=1
J=1/2
Upper limit J=0
3.5
4.0
4.5
5.0
5.5
W (GeV)

FIG.8

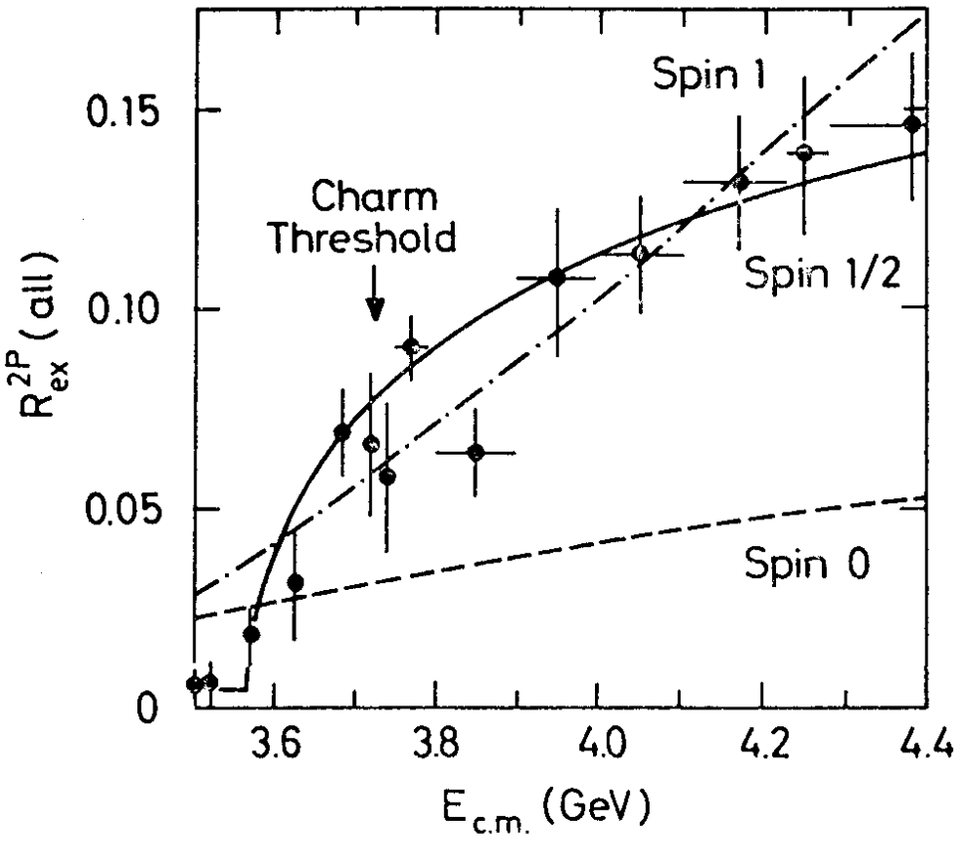
Spin 1
Charm
Threshold
Spin 1/2
Spin 0
0.15
0.10
0.05
0
R_{ex}^{2P} (all)
3.6
3.8
4.0
4.2
4.4
$E_{c.m.}$ (GeV)

FIG.9

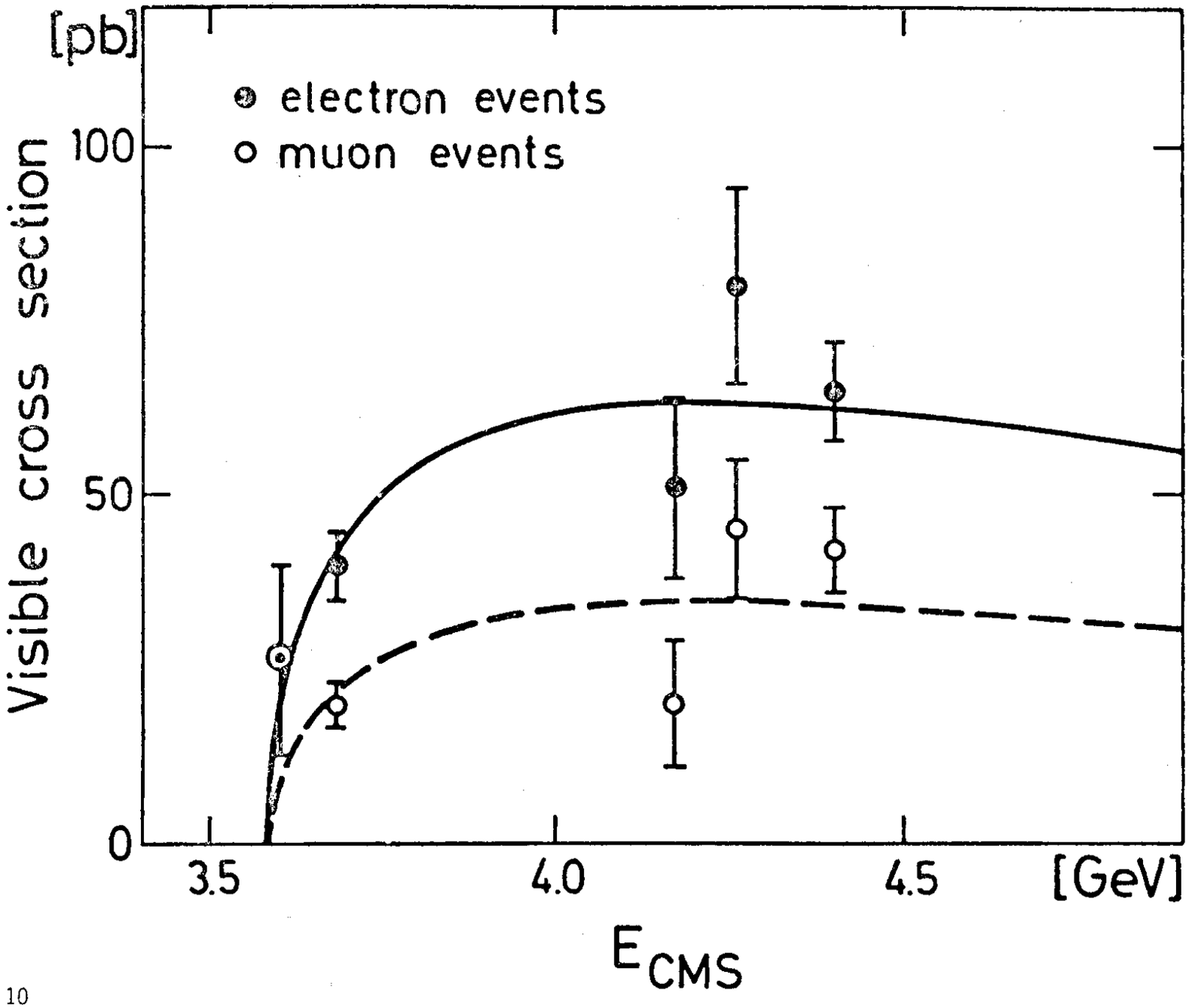
[pb]
electron events
muon events
Visible cross section
100
50
0
3.5
4.0
4.5
[GeV]
E_{CMS}
28039

FIG.10

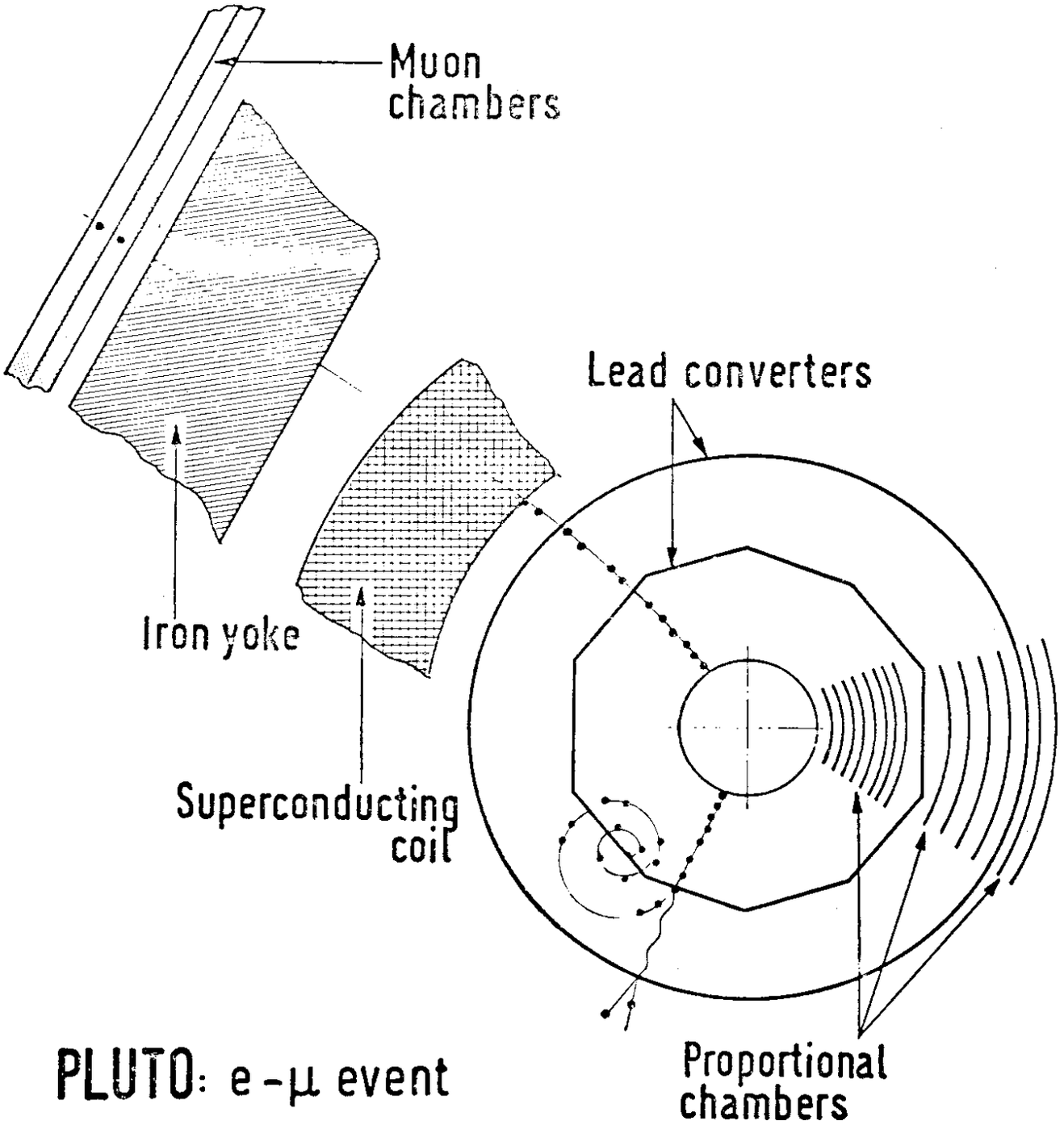

PLUTO: e - μ event

FIG.11

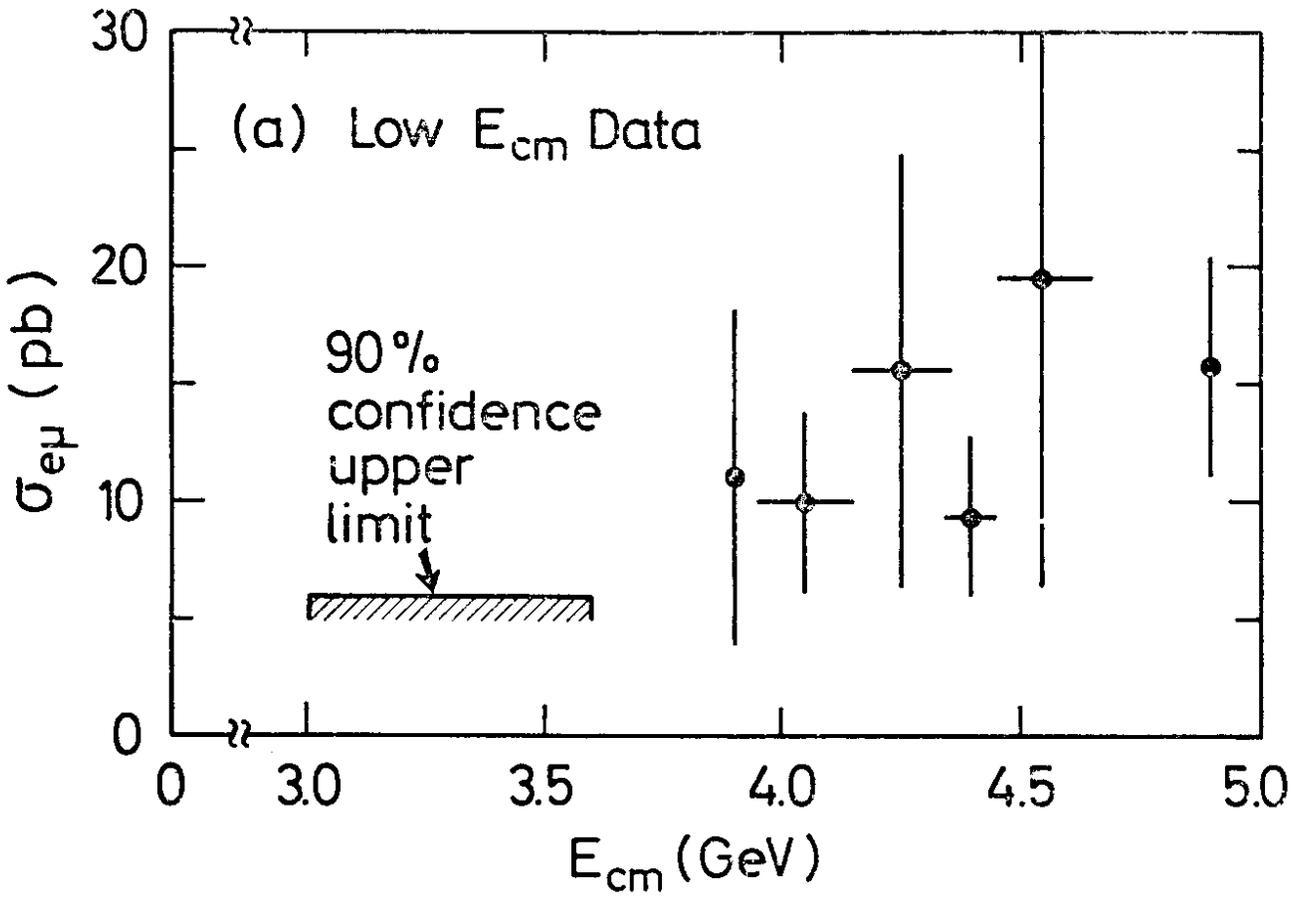
(a) Low E_{cm} Data
90% confidence upper limit
$\sigma_{e\mu}$ (pb)
E_{cm} (GeV)
0
10
20
30
3.0
3.5
4.0
4.5
5.0

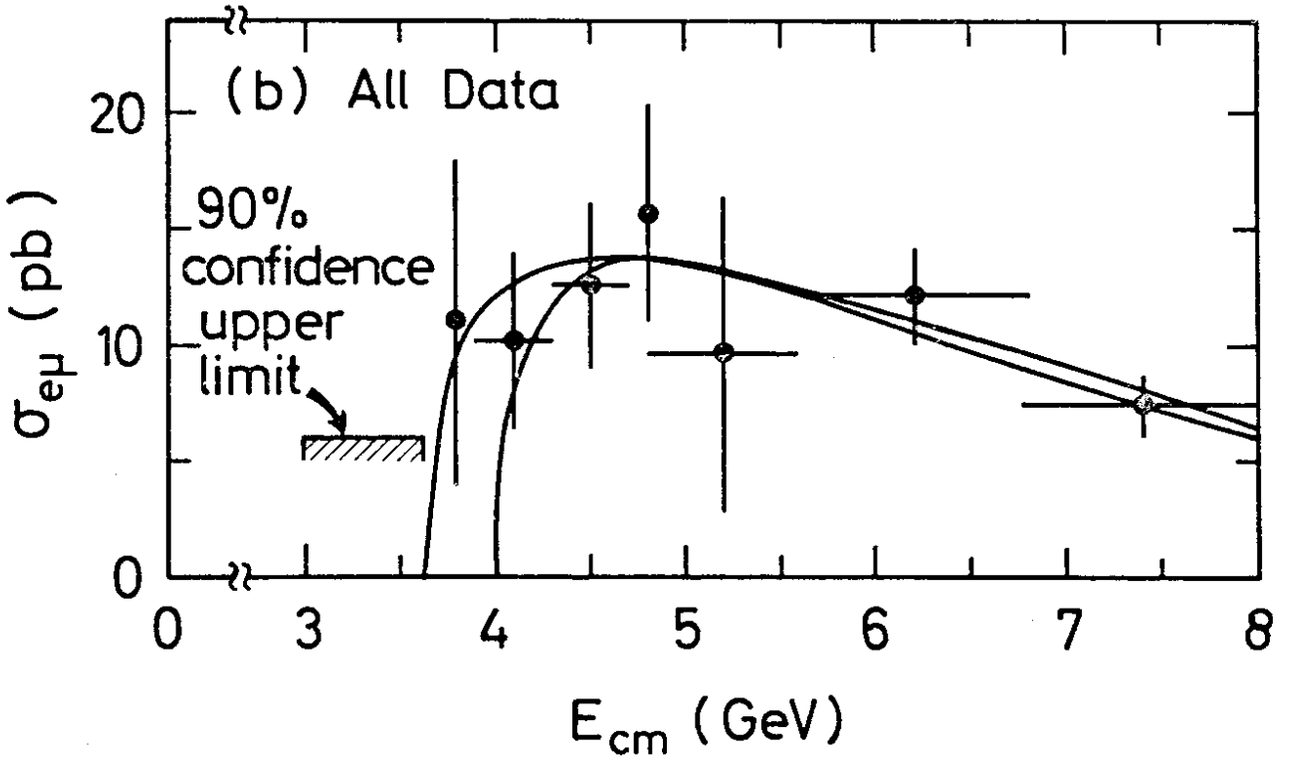
(b) All Data
90% confidence upper limit
$\sigma_{e\mu}$ (pb)
E_{cm} (GeV)
0
10
20
3
4
5
6
7
8

FIG.12

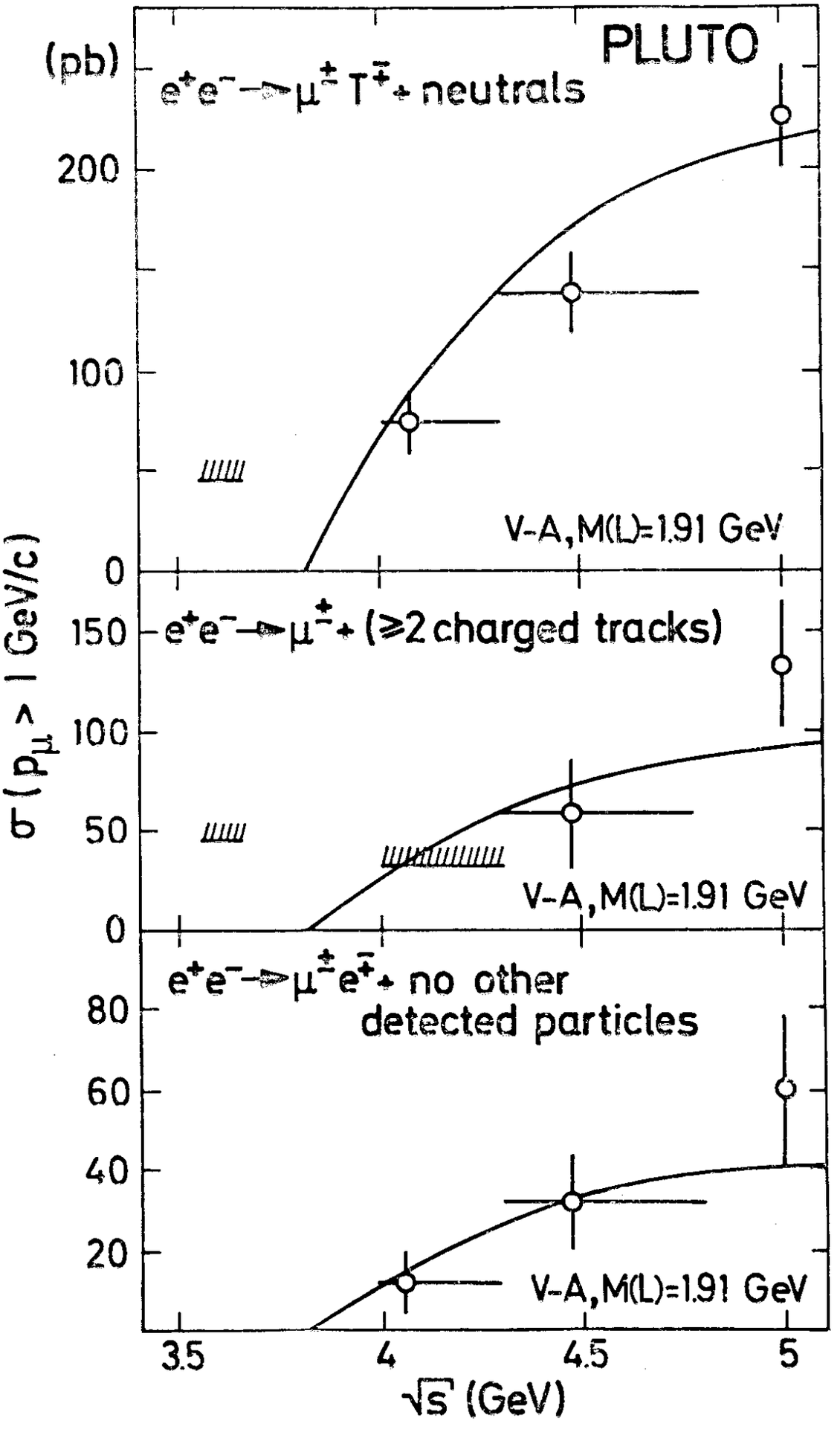
PLUTO
(pb)
$e^+e^- \to \mu^\pm \tau^\mp$ + neutrals
200
100
0
V-A, M(L)=1.91 GeV
$e^+e^- \to \mu^\pm$ + (≥2 charged tracks)
150
100
50
0
V-A, M(L)=1.91 GeV
$e^+e^- \to \mu^\pm e^\mp$ + no other detected particles
80
60
40
20
V-A, M(L)=1.91 GeV
$\sigma(p_\mu > 1\ GeV/c)$
3.5
4
4.5
5
$\sqrt{s}$ (GeV)

FIG.13

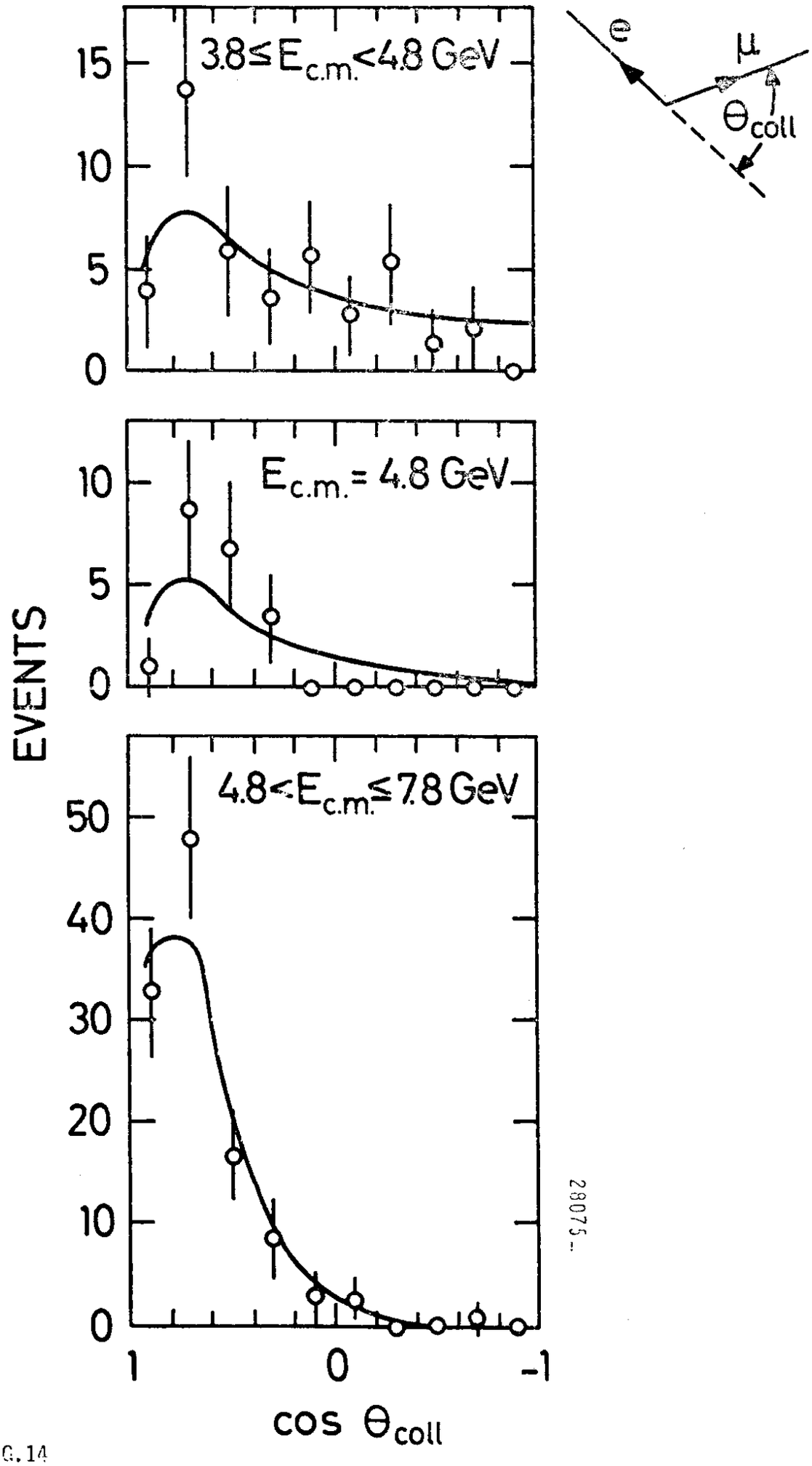
3.8≤E c.m.<4.8 GeV
E c.m. = 4.8 GeV
4.8<E c.m.≤7.8 GeV
EVENTS
cos θ coll
e
μ
θ coll
28075-

FIG.14

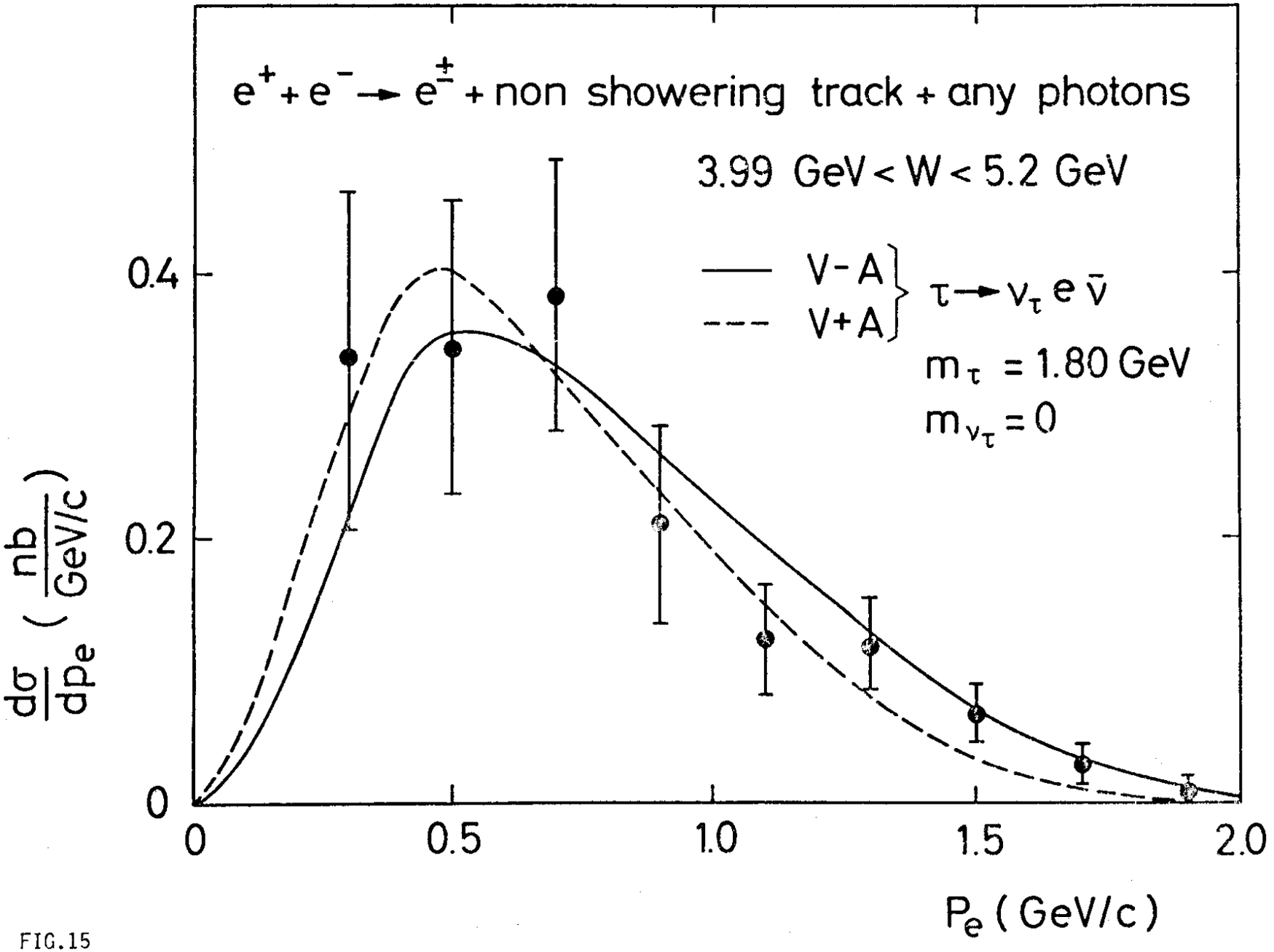
$e^+ + e^- \rightarrow e^{\pm}$ + non showering track + any photons
3.99 GeV < W < 5.2 GeV
V-A
V+A
$\tau \rightarrow \nu_\tau e \bar{\nu}$
$m_\tau = 1.80$ GeV
$m_{\nu_\tau} = 0$
$\frac{d\sigma}{dp_e}$ ($\frac{nb}{GeV/c}$)
0
0.2
0.4
0
0.5
1.0
1.5
2.0
P_e (GeV/c)

FIG.15

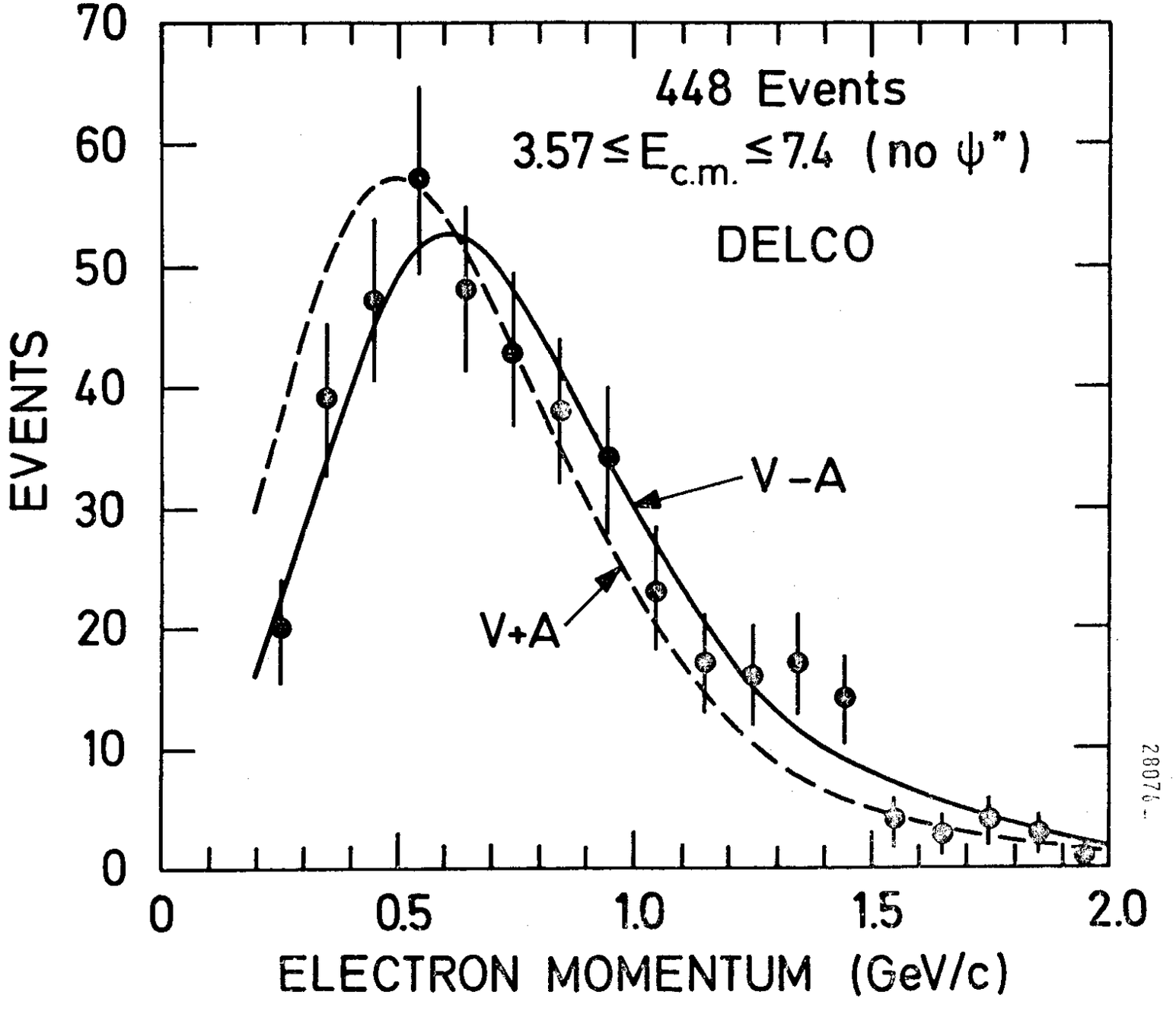
448 Events
3.57 ≤ E c.m. ≤ 7.4 (no ψ")
DELCO
V-A
V+A
EVENTS
ELECTRON MOMENTUM (GeV/c)
0
10
20
30
40
50
60
70
0
0.5
1.0
1.5
2.0
28076

FIG.16

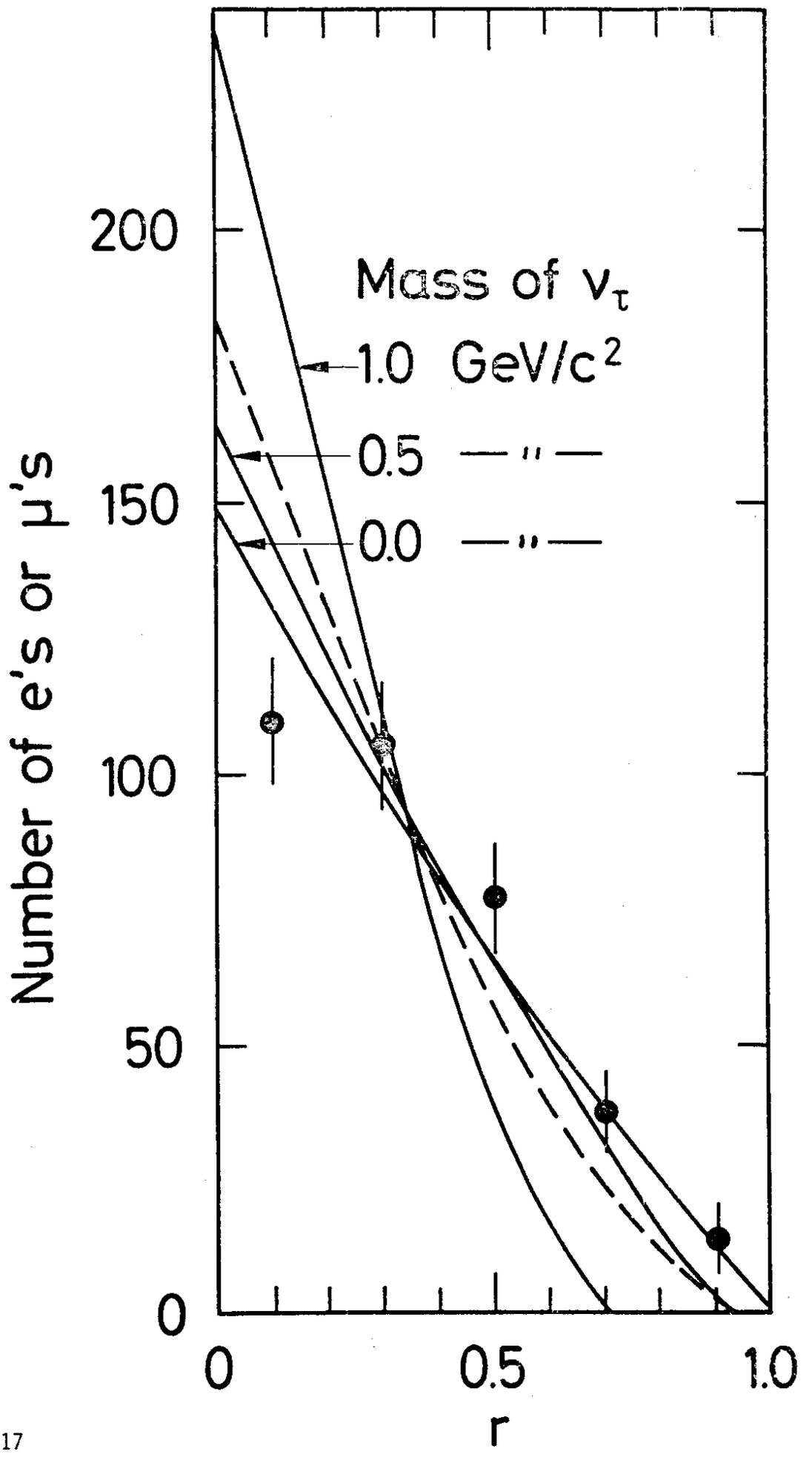
Mass of ν_τ
1.0 GeV/c^2
0.5 — " —
0.0 — " —
Number of e's or μ's
200
150
100
50
0
0
0.5
1.0
r

FIG.17

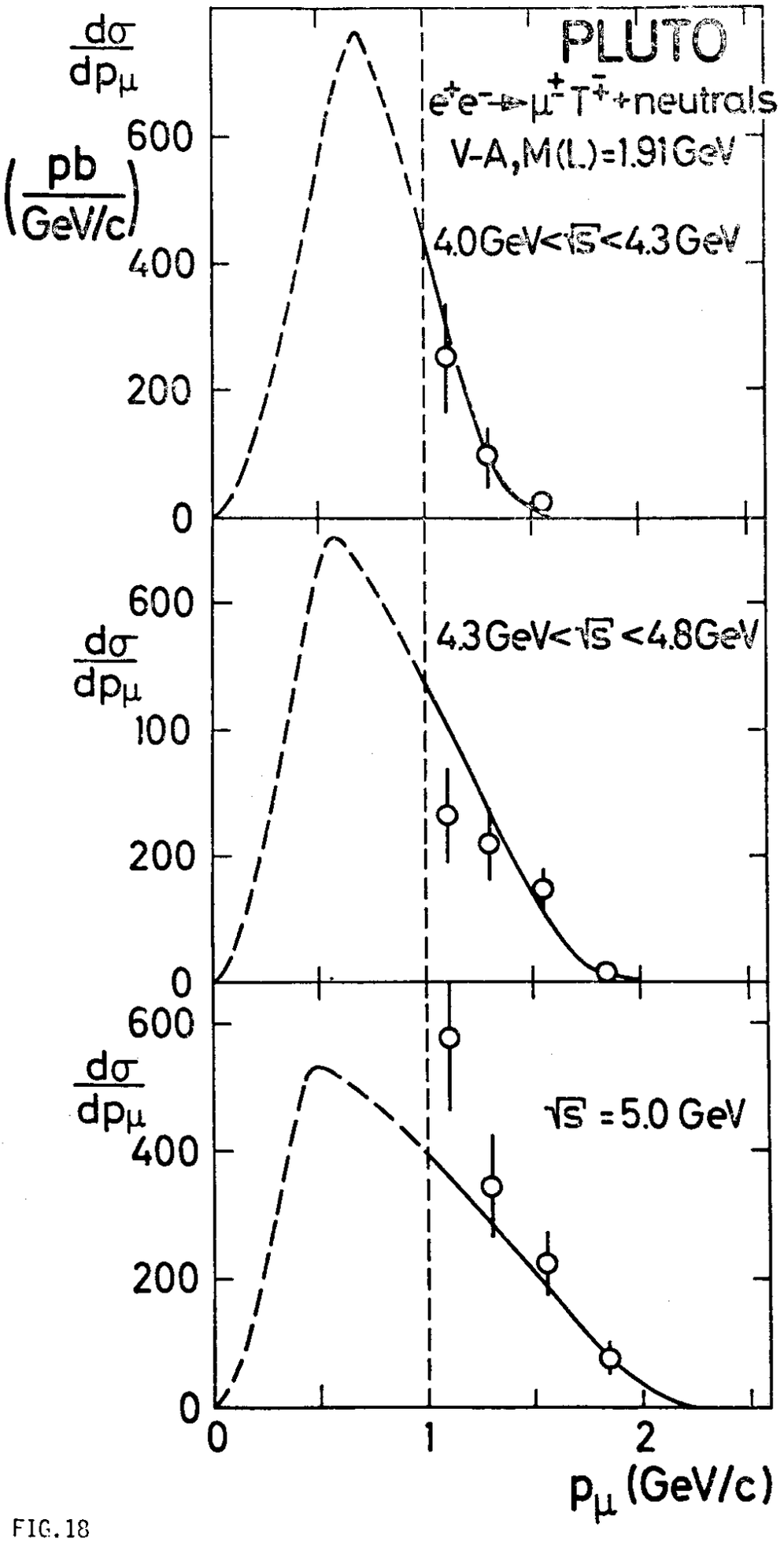
PLUTO
$e^+e^- \to \mu^+ T^- +$ neutrals
V-A, M(L.)=1.91 GeV
4.0 GeV < √s < 4.3 GeV
4.3 GeV < √s < 4.8 GeV
√s = 5.0 GeV
$\frac{d\sigma}{dp_\mu}$
$\left(\frac{pb}{GeV/c}\right)$
600
400
200
100
0
1
2
p_μ (GeV/c)

FIG. 18

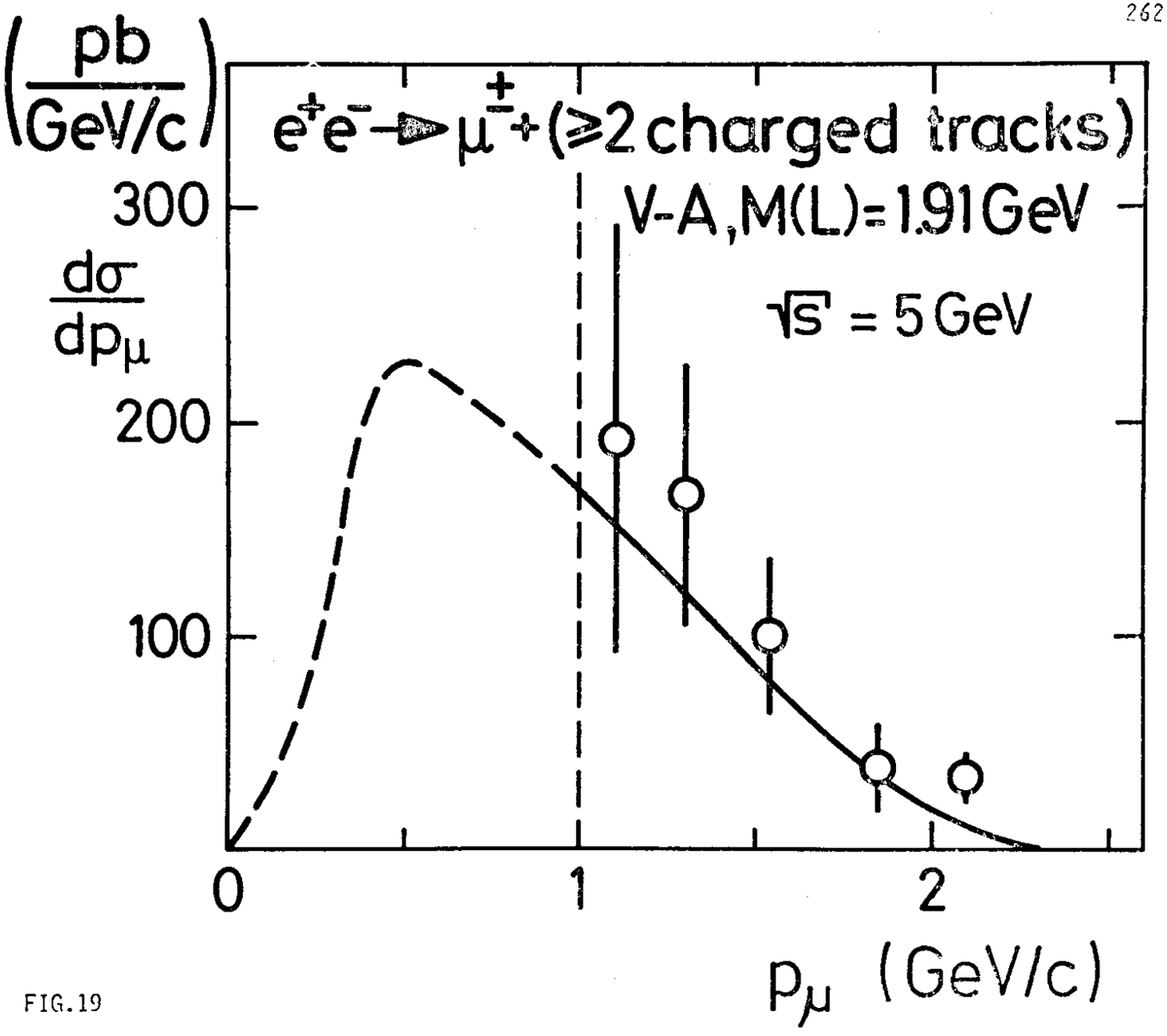
(pb/GeV/c)
$e^+e^- \rightarrow \mu^\pm +$ (≥2 charged tracks)
V-A, M(L)=1.91 GeV
$\sqrt{s}$ = 5 GeV
$\frac{d\sigma}{dp_\mu}$
300
200
100
0
1
2
p_μ (GeV/c)

FIG.19

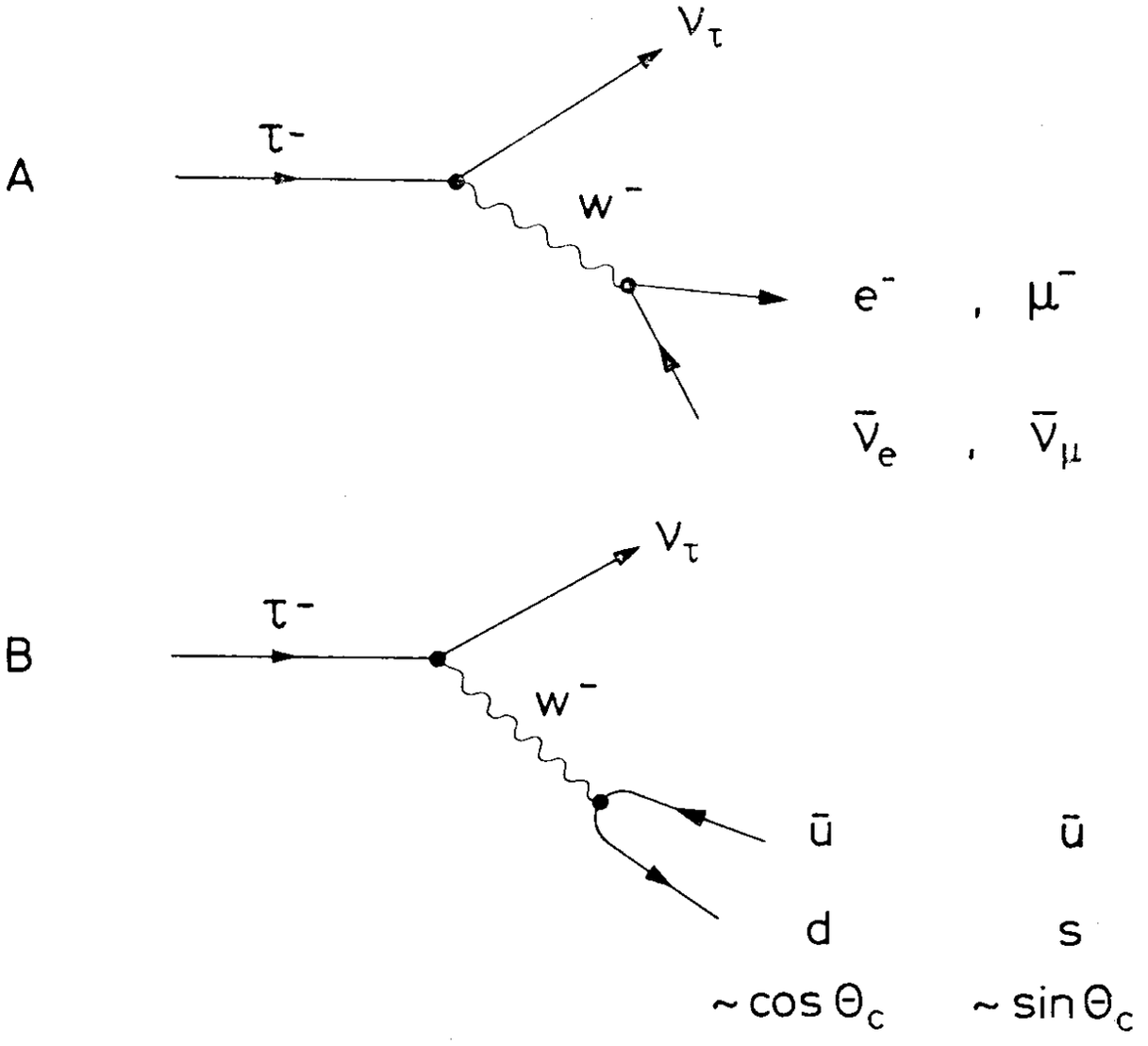
A
τ^-
ν_τ
w^-
e^- , μ^-
$\bar{\nu}_e$, $\bar{\nu}_\mu$
B
τ^-
ν_τ
w^-
$\bar{u}$ $\bar{u}$
d s
$\sim \cos\Theta_c$ $\sim \sin\Theta_c$
C
τ^-
ν_τ
w^-
π^-
g
$gf_\pi \cdot \cos\Theta_c$
D
π^-
w^-
$\bar{\nu}_\tau$
$gf_\pi \cdot \cos\Theta_c$
g
μ^-

FIG.20

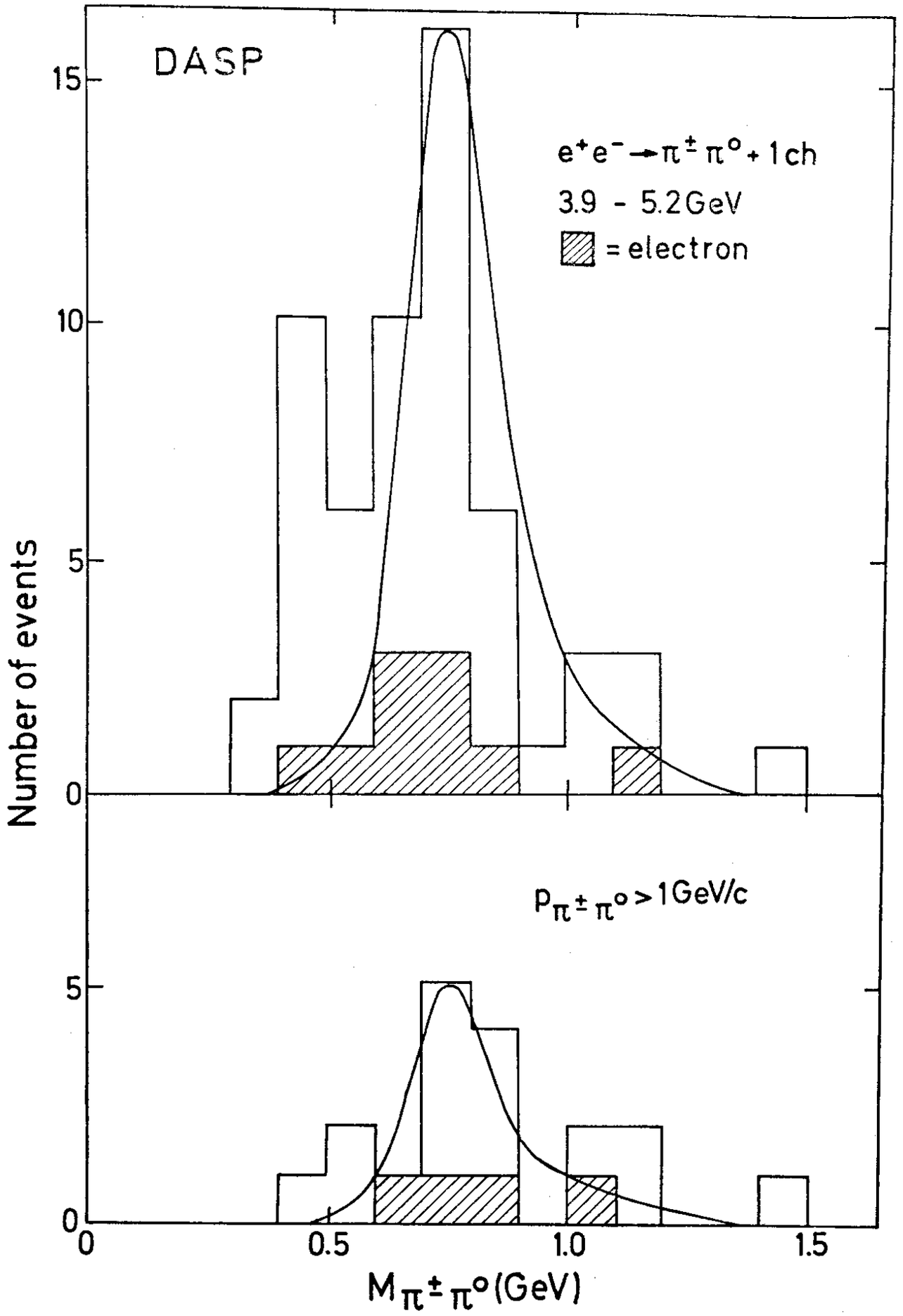
DASP
$e^+e^- \rightarrow \pi^\pm \pi^o + 1ch$
3.9 - 5.2GeV
= electron
$p_{\pi^\pm \pi^o} > 1GeV/c$
Number of events
$M_{\pi^\pm \pi^o}$(GeV)
0
5
10
15
0.5
1.0
1.5

FIG.21a

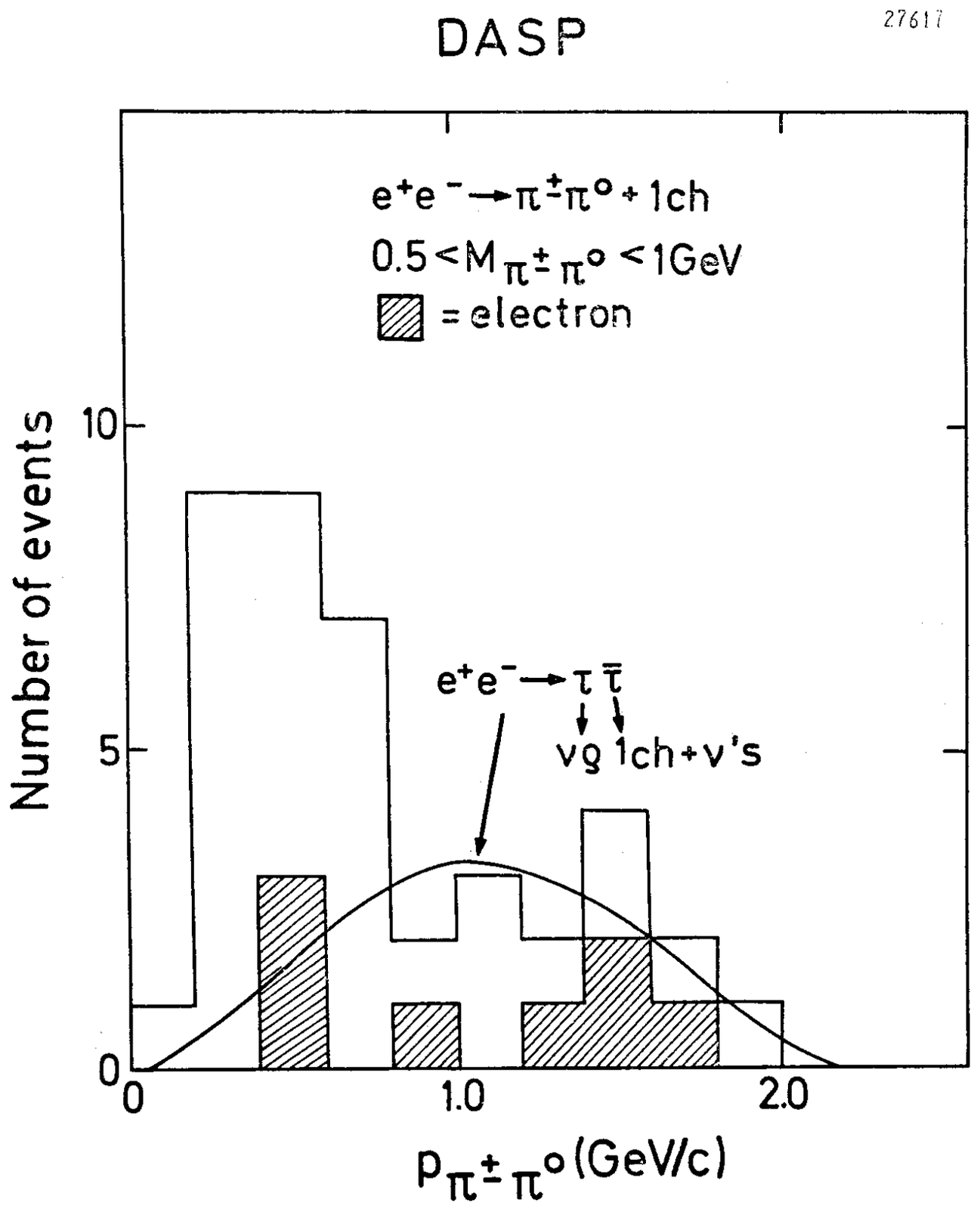
DASP
$e^+e^- \rightarrow \pi^\pm\pi^o + 1ch$
$0.5 < M_{\pi^\pm\pi^o} < 1GeV$
= electron
$e^+e^- \rightarrow \tau\bar{\tau}$
ν_τ 1ch+ν's
Number of events
10
5
0
0
1.0
2.0
$p_{\pi^\pm\pi^o}$ (GeV/c)

FIG.21b

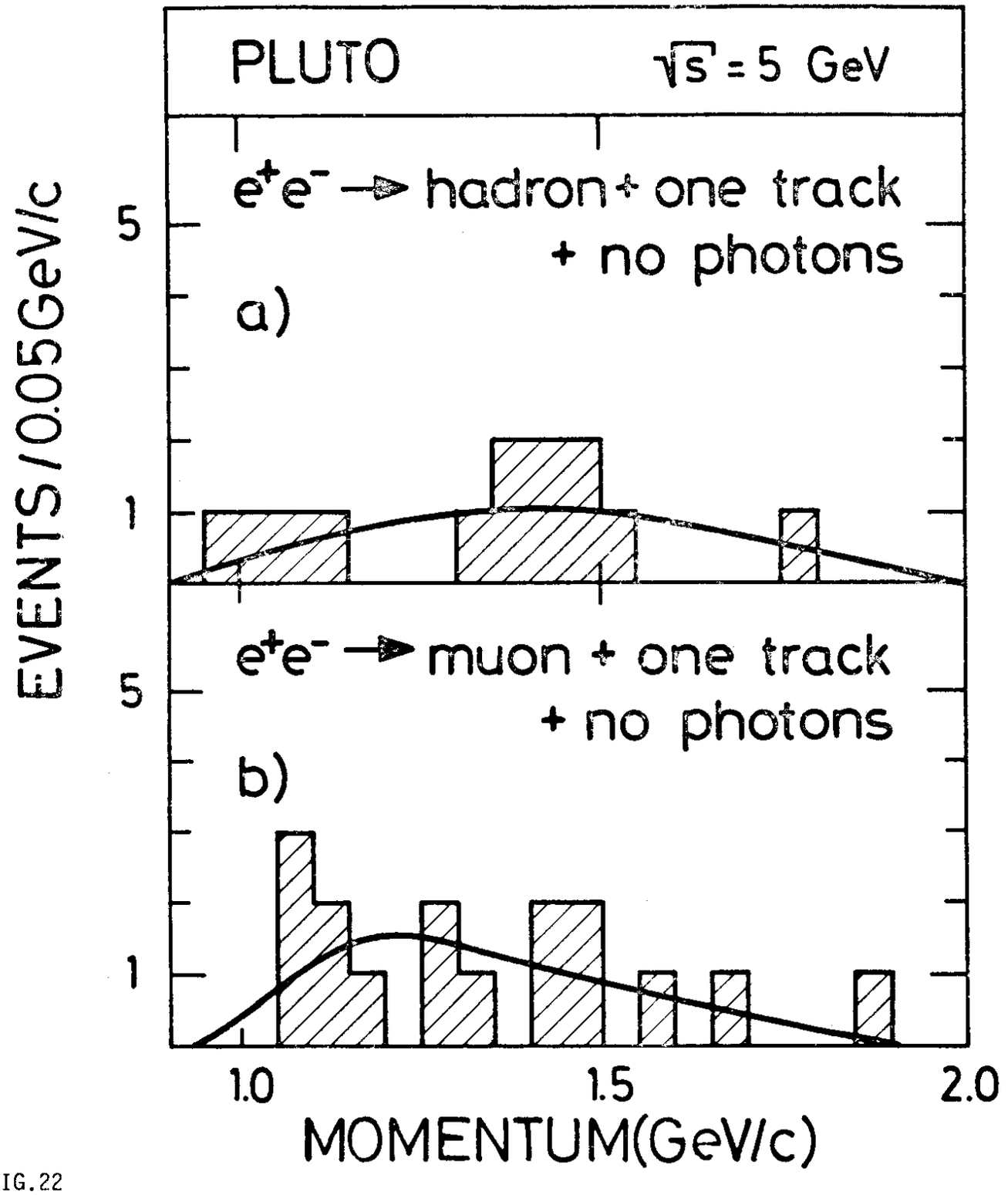
PLUTO
√s = 5 GeV
e+e- → hadron + one track
+ no photons
a)
e+e- → muon + one track
+ no photons
b)
EVENTS/0.05GeV/c
5
1
5
1
1.0
1.5
2.0
MOMENTUM(GeV/c)

FIG.22

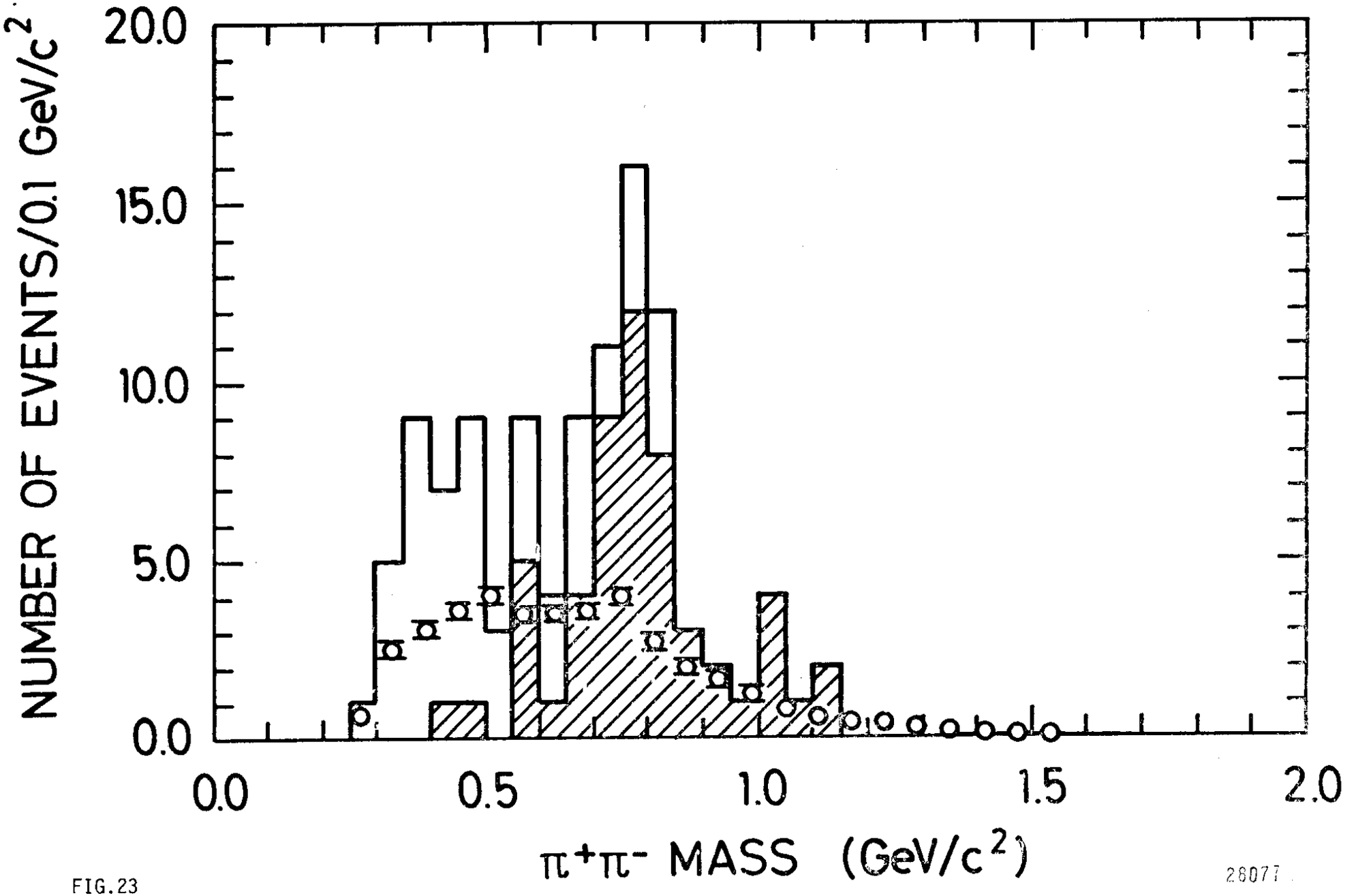
NUMBER OF EVENTS/0.1 GeV/c²
20.0
15.0
10.0
5.0
0.0
0.0
0.5
1.0
1.5
2.0
π⁺π⁻ MASS (GeV/c²)

FIG.23

26077

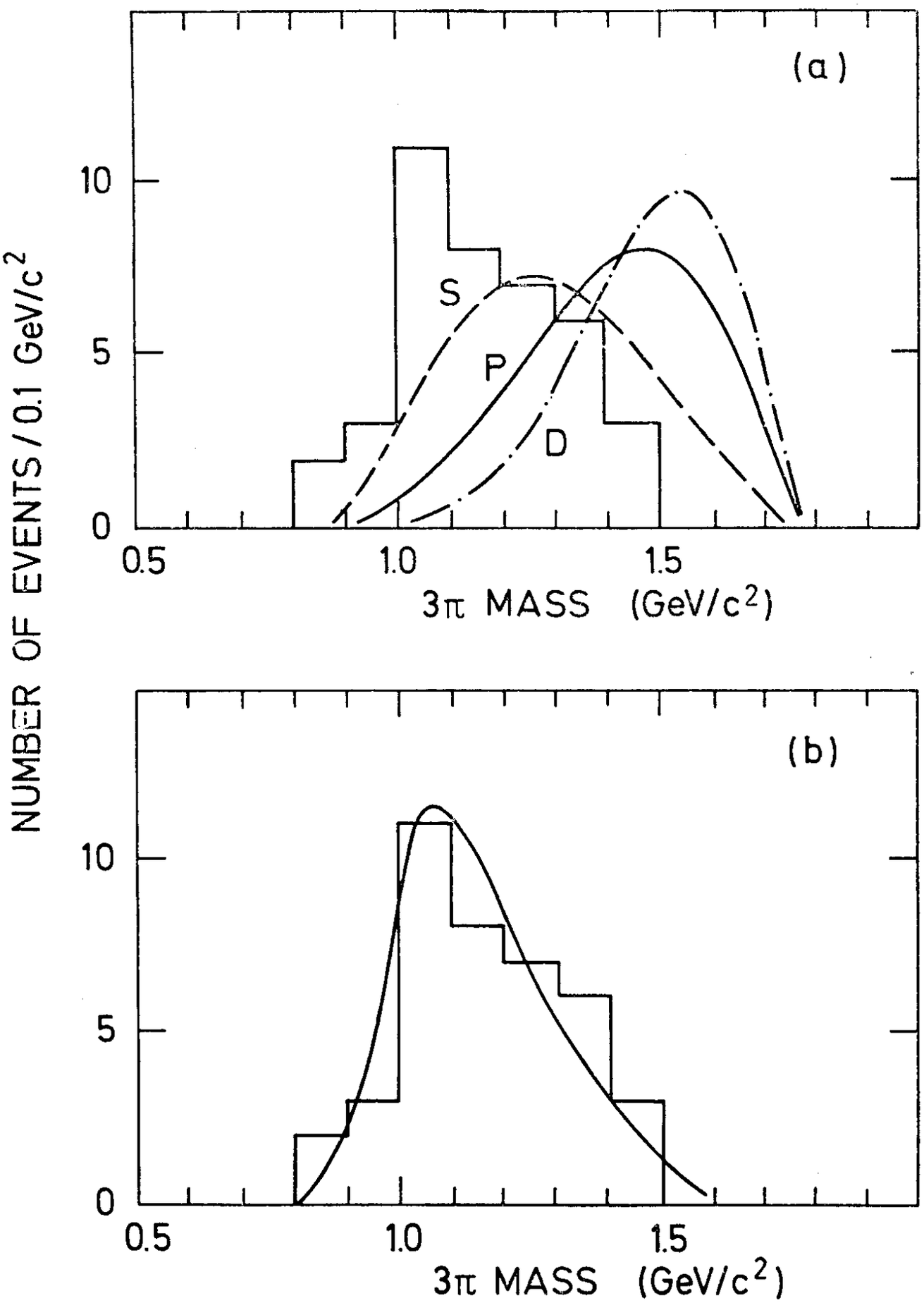
(a)
S
P
D
10
5
0
0.5
1.0
1.5
3π MASS (GeV/c²)
NUMBER OF EVENTS / 0.1 GeV/c²
(b)
10
5
0
0.5
1.0
1.5
3π MASS (GeV/c²)

FIG.24

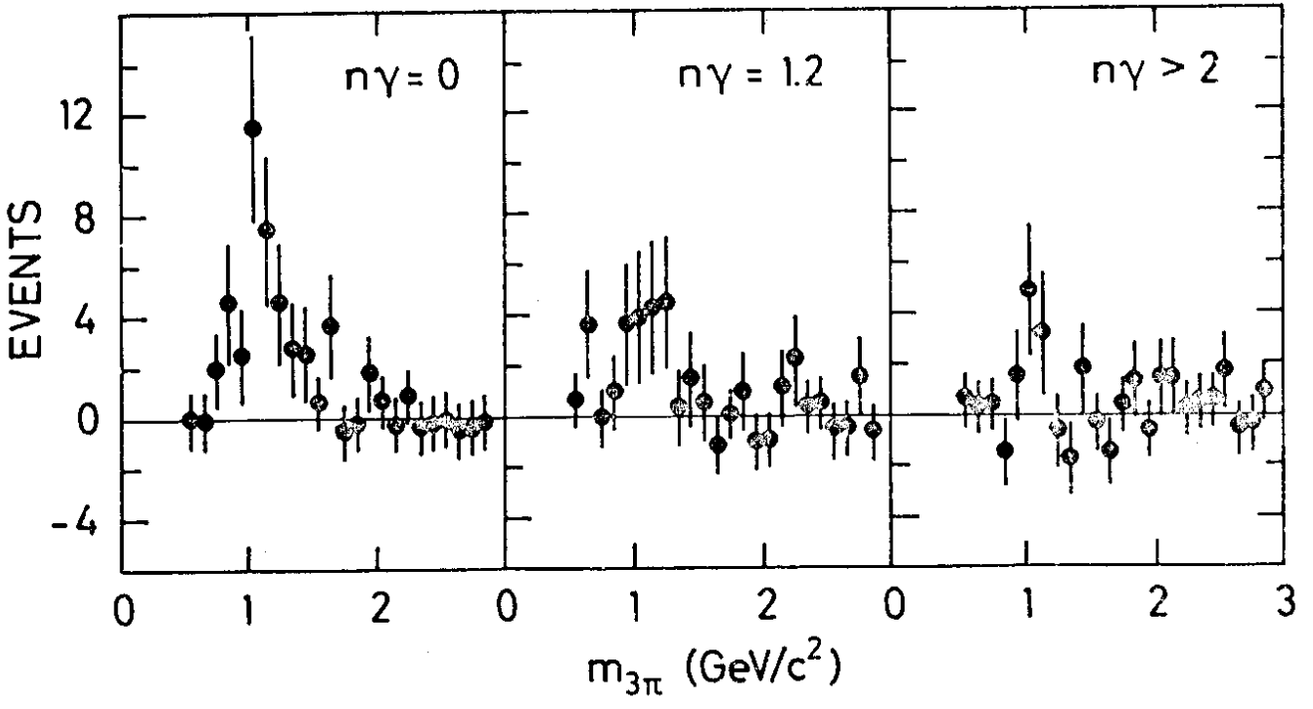

FIG.25